ELSEVIER

Tectonophysics 333 (2001) 293–322

TECTONOPHYSICS

www.elsevier.com/locate/tecto

Deformation history of the southwestern Taiwan foreland thrust belt: insights from tectono-sedimentary analyses and balanced cross-sections

F. Mouthereau[a,*], O. Lacombe[a], B. Deffontaines[a], J. Angelier[a], S. Brusset[b]

[a]*Département de Géotectonique, ESA 7072, Université Pierre et Marie Curie, T.26-25, E1, Case 129, 4, place Jussieu 75252 Paris Cedex 05, France*

[b]*Dynamique des bassins, 38, rue des 36-ponts 31400 Toulouse, France*

Received 11 August 1999; revised 24 February 2000

Abstract

Analysis of the basin-scale and local deformation history and estimates of shortening rates are performed in the southwestern foreland thrust belt of the Plio-Pleistocene Taiwan orogen. Timing of deformational events is constrained using both syntectonic unconformities and other markers of syndepositional tectonic activity. Three cross-sections are investigated and balanced. Intermediate shortening rates are estimated based on balanced and restored cross-sections. The total amount of shortening along studied balanced sections results from superimposed thin-skinned and thick-skinned styles. A shallow aseismic thick décollement is located to depth of 6–8 km at the base of thick Late Miocene shales that behaves as ductile layer. The occurrence of a deep seismic décollement to depth of 12–15 km is confirmed by seismicity, fault plane solutions of focal mechanisms and a seismic reflection profile providing evidence of reactivated and inverted inherited extensional features beneath the Coastal Plain. Three major tectonic stages are recognized within the southwestern Foothills, which are correlated with local thrusting events. The first stage begins at 5 Ma with the onset of the Taiwan collision and ends at 2–1.6 Ma. It reflects an initial submarine accretionary stage associated with moderate tectonic activity. The second major stage occurs during Late Pliocene–Early Pleistocene. This "intermediate" collision stage sealed the evolution of the southern foreland thrust wedge from submarine to continental environment in relation with exhumation and denudation of the Central Range. The last stage of deformation begins in the Middle Pleistocene and continues until present. It is associated with high rates of sedimentation and most of the thrusts are activated or reactivated at that time and out-of-sequence thrusting occurs. The collision started synchronously near 5 Ma throughout the southwestern Taiwan. Total and intermediate shortening rates are more or less constant through time in studied sections; that may suggest that long-term deformation in the Taiwan foreland thrust belt occurred more or less at steady-state. Since 5 Ma, the southward decrease of rates of shortening from 3.6 to 4.8 mm/year in northern sections to 2.2 mm/year in southern section might be related to both influence of indentation by the Peikang High to the north and southward transition, at the scale of the southwestern Foothills, from collision to subduction setting; the effect of the obliquity of the convergence resulting in regional southward migration of the collision cannot be definitely inferred from this analysis. Our results place new kinematic and time constraints, which must be taken into account in forthcoming geodynamic models of the Taiwan collision.

Keywords: balanced cross-sections; syntectonic deposits; shortening rates; foreland thrust belt; Taiwan

* Corresponding author.
E-mail address: frederic.mouthereau@lgs.jussieu.fr (F. Mouthereau).

0040-1951/01/$ - see front matter
PII: S0040-1951(00)00280-8

1. Introduction

For many years, the Taiwan Mountain Belt has been presented as a key example for understanding the evolution of active foreland thrust belts. Preliminary geological studies focused on the structure of some particular areas of the western frontal units (Suppe, 1976, 1980; Namson, 1981) and led to general concepts on the theoretical geometry of thrust-related folds in folded belts (Suppe, 1983). These former concepts were extended to the entire Taiwan orogen and inspired the earliest modeling of the mountain range based on critical wedge theory and thin-skinned tectonics (Suppe, 1981; Davis et al., 1983). Recent geophysical data such as gravity (Ellwood et al., 1996; Yen et al., 1998) or seismic tomography (Wu et al., 1997) have allowed to greatly improve our representation of the Taiwan orogen in terms of crustal-scale thick-skinned deformation. Furthermore, geodetic measurements derived from the Taiwan GPS Network survey (Yu et al., 1997) and the recalculation of new focal mechanisms (Wu et al., 1997; Kao et al., 1998) provided additional constraints on the kinematics and the mechanical behavior of the crust during arc–continent collision.

Recent evidence of structural inversion beneath the Coastal Plain and offshore basins have led to revisit the classic model of thin-skinned deformation in the Western Foothills of Taiwan and to discuss thin-skinned vs thick-skinned tectonics styles in this region (Chang et al., 1996; Hung et al., 1999; Mouthereau et al., 1999, 2001). Preliminary investigations of the Neogene kinematics of the Taiwan foreland thrust belt by means of estimates of shortening rates (Mouthereau et al., 1996) have emphasized a significant decrease of shortening rates from north (11 mm/year) to south (2 mm/year) during the last 1.6 Ma, interpreted as a consequence of the obliquity of the convergence and related southward migration of the maximum collisional shortening through time.

This study focuses on the tectono-sedimentary history of the southwestern Taiwan foreland in the framework of the overall evolution of the Taiwan Mountain Range. We first attempt at estimating shortening rates in the southwestern Foothills based on a tectono-sedimentary analysis of syntectonic deposits that provides ages of individual thrust initiation and reactivation. Then, using these time constraints we balance and restore three cross-sections using LOCACE® software from which we determine the total amount of shortening along the studied sections. Then, based on the sequential analysis of deformation we estimate total and intermediate time-averaged shortening rates along sections since individual thrusts have been activated.

2. Southwestern Taiwan: kinematics and structural setting

The active Taiwan mountain belt results from the oblique Plio-Quaternary collision between the Philippine Sea Plate (i.e. the Luzon Arc) and the Eurasian block of South China (i.e. the Chinese continental margin) (Fig. 1). According to recent GPS survey (Yu et al., 1999), the present-day convergence rate of the Luzon arc with respect to the Chinese margin is about 8 cm/year across the active Taiwan orogen. The continental margin is oriented N60°E whereas the rigid Luzon arc strikes N10°E and moves in a N58°W direction. The resulting convergence vector is oblique, at an angle of 28°. In response to this obliquity, the collision in Taiwan propagates southward (Suppe, 1981, 1984). Assuming that this situation prevailed since the Pliocene until the present, the southwestern foreland thrust belt should be one of the less intensely deformed parts of the Foothills.

Within the framework of the western Taiwan foreland thrust belt, the southwestern foreland province is located in a transitional domain between the Taiwan collision belt sensu stricto to the north and the Manila accretionary domain to the south. Along the strike of the orogen the transition is outlined by the occurrence of two distinct seismic domains abruptly separated by a WNW–ESE-trending feature (Lacombe et al., 2001). At the scale of the Western Foothills, further structural investigations (Mouthereau et al., 2001) demonstrate that basement-involved deformation and inversion tectonics occur north of this WNW–ESE feature, arguing in favor of ongoing collision enhanced by the foreland indentation of the Peikang basement high. In contrast, to the south, few earthquakes occur, and this lack of seismicity might be attributed to the incipient collision or accretionary prism setting. At the surface, this major oblique zone was defined by morphostructural analysis and

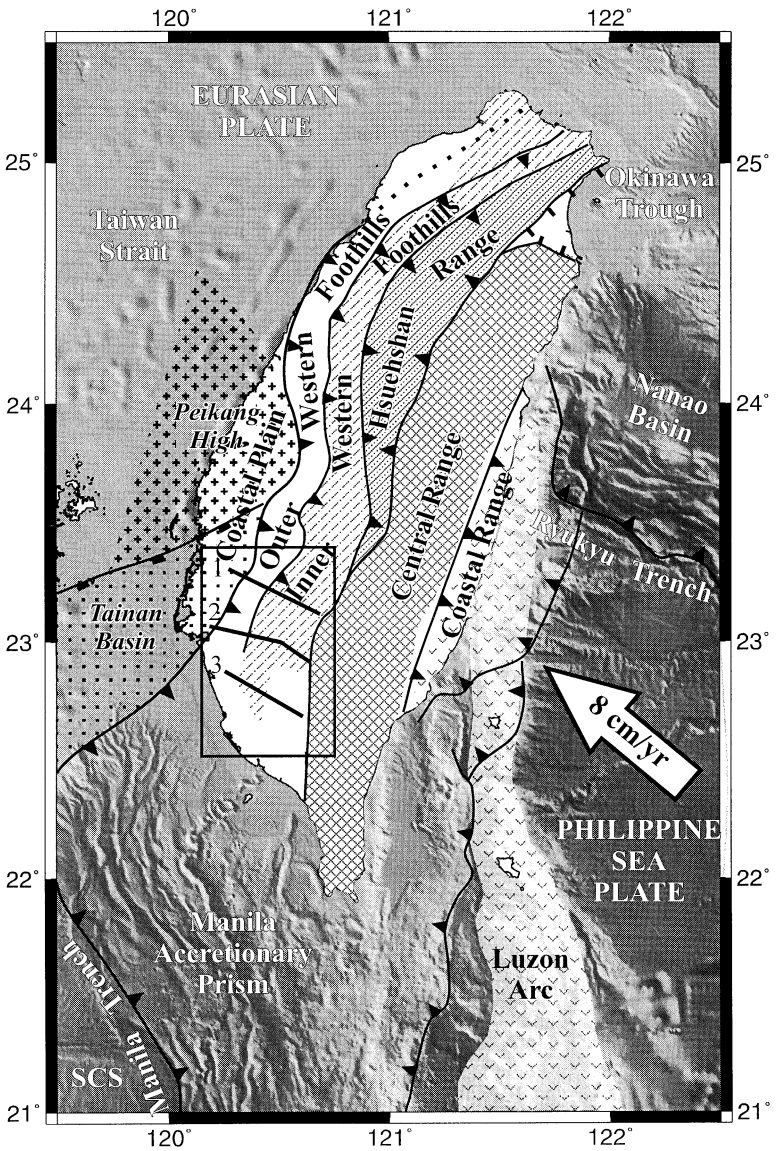

Fig. 1. Geodynamic setting and major geological features of the Taiwan Mountain Range. The study area is located in the southwestern Foothills at the transition between the Taiwan foreland thrust belt and Manila Accretionary Prism. The geological cross-sections presented in this work are, respectively, (1) Yushing, (2) Kuanmiao and (3) Alien sections.

was called the Chishan Transfer Fault Zone (CTFZ) by Deffontaines et al. (1997); its kinematics and geological significance have been recently studied and discussed by Lacombe et al. (1999). Furthermore, the results of geodetic retriangulation within the orogen (Chen, 1984) demonstrates that the area north of the CTFZ is characterized by uplift whereas to the south subsidence prevails. Additional analyses of paleostress patterns in the frontal units of southwestern Taiwan (Angelier et al., 1986; Rocher et al., 1996; Lacombe et al., 1997, 1999; this work) have led to determine an average N100–110E shortening compatible with the main thrust orientations.

3. Timing of deformation in southwestern thrust wedge by analysis of syntectonic deposits

3.1. Tectonic history of the Taiwan foreland

Three major regional unconformities can be distinguished within the western foreland of Taiwan in the vicinity of the Peikang High and within the Tainan Basin (Fig. 1) that outline the major trends of the tectonic evolution of the southern Taiwan region.

The first major unconformity, Late Oligocene–Early Miocene in age, may be correlated either to a change in spreading direction from N–S to NW–SE that occurred near 20 Ma in the South China Sea (Pautot et al., 1986) or to a post-rift unconformity as it was suggested by Yu and Chou (1999). It is beyond the scope of this study to discuss both interpretations since they do not concern the collisional history of the rifted Chinese margin.

A second unconformity has been recognized within the Middle–Late Miocene at 8–12 Ma. This unconformity is particularly well observed in the vicinity and toward the center of the Peikang High, which led Chang and Chi (1983) to interpret it as the record of the tectonic uplift of the Peikang basement high at that time. This episode is followed by an important transgression stage at 8 Ma and deposition of shallow-marine sediments of the Kueichulin formation in northern Taiwan. Within the Tainan basin, Lee et al. (1993) correlate this Middle–Late Miocene unconformity with superimposed structural inversion and thermal subsidence as shown by the basement subsidence curves. Earlier studies (Lu and Hsü, 1992; Déramond et al., 1996) previously interpreted the 8 Ma unconformity as the record of a first collision in Taiwan prior to the Plio-Pleistocene collision. On the opposite, Teng (1990) considers that the Luzon arc began to override the Asian continental margin in the late Middle Miocene (about 12 Ma) during an early stage of the Plio-Pleistocene collision. Furthermore, the Peikang high, i.e. the Chinese continental margin, experienced a change of extensional directions from N–S to NW–SE near 8–9 Ma (Angelier et al., 1990), which might be related to the early and wide response of the Chinese margin to collisional flexure. In the light of the previous arguments, it is not necessary to invoke an early collision near 8 Ma. We propose to interpret the 8–12 Ma unconformity as the result of an initial basement bulge (forebulge?) beneath the Coastal Plain accompanying the initiation of the foreland basin. In this view, it may be considered as reflecting a first record of the transition from Chinese passive margin to collision-related setting.

The onset of the true collision is outlined by the beginning of the well-marked flexural subsidence at about 4–5 Ma in the northern (Chi and Huang, 1981; Yu and Teng, 1988) as well in the southern foreland (Lee et al., 1993). The foreland basin is progressively filled in by synorogenic sediments that unconformably overlie (progressive onlaps) the Miocene deposits. This defines a foreland unconformity increasing toward the Peikang high (Yu and Chou, 1999).

The Miocene rocks are progressively thicker to the south (Ho, 1988) and gradually change from littoral and deltaic facies associated with coal and basaltic tuffs in the north, to shallow-marine facies and even deep marine environments to the south. The Pliocene rocks correspond more or less to shallow-marine marine clastic deposits thickening toward the south. The thick Pleistocene formations exposed in lowlands of the western Foothills form a prograding sedimentary wedge of synorogenic deposits: they reflect the transition through time from deep offshore marine deposits, shallow-marine, lagoonal and finally to fluvial and non-marine deposits.

The main characteristics of the sedimentation in the Western Foothills are the rapid lateral (in space) and vertical (in time) changes of facies which imply that the names of formations changed laterally north–south because of the southward deepening of the flexed margin and east–west from inner to external domains of the Foothills due to the syndepositional tectonics. However, the compilation of stratigraphic data and age connection between wells drilled in the foreland has allowed correlation problems to be solved (Shaw, 1996).

3.2. Tectono-sedimentary analysis of the southwestern thrust belt

The problem of the relation between tectonic evolution and sedimentation has been extensively investigated through the last 10 years in foreland thrust belts such as the Pyrenees (Puigedefabregas et al., 1992) or the Himalayan foredeep (Burbank and Raynolds, 1988). The western foreland basin of Taiwan has

been also preliminarily documented in terms of tectono-sedimentary analysis (Covey, 1984, 1986; Delcaillau et al., 1993; Déramond et al., 1996).

The first-order stratigraphic architecture observed in a foreland is controlled by large-scale deflection of the underlying basement produced in response to the tectonic loading of the orogen (Beaumont, 1981). As deformation propagates westwards, the basin is affected by thrusting, thus providing a second-order control on the foreland stratigraphy. At the scale of the flexural basin, the evolution of the foreland could be viewed as the result of the growth of a prograding sedimentary wedge onto a passive margin in response to crustal loading. This corresponds classically to the *flysh* to *molasse* transition found in the northern Alps (Sinclair, 1997) or deep-water to shallow-marine and continental sedimentary transition in the Taiwan foreland (Covey, 1986). At the scale of a foreland thrust system, this general trend is altered by the progressive migration of syntectonic depocenters (Puigedefabregas et al., 1992) within the foreland and more locally by local thrust sheet loading and related fold uplift.

Déramond et al. (1996) preliminary described the timing of thrusting along two sections of the Taiwan foreland on the basis of sequential stratigraphy analysis of synorogenic deposits. As these authors pointed out, the use of sequential stratigraphy to date thrust activity supposes that sea-level fluctuations recorded by facies variations of marine synorogenic deposits are either controlled by tectonism or mainly driven by eustatism but nevertheless enhanced by tectonism. At the basin scale, from the orogenic front to the forebulge, the effect of eustatism on stratigraphic record, e.g. the distribution of facies and location of unconformities, could be distinguished from the effect of episodic tectonism as revealed by modeling (Jordan and Flemings, 1991). Nevertheless, at the scale of a thrust unit, it should be much more difficult to separate eustatic and tectonic influence on the sedimentary record because at the scale of few kilometers, the parameters used in the modeling (erosion, deposition, subsidence and amount of shortening) are (1) not easily assessable and (2) likely to poorly modify the depositional system over large areas.

A tectono-sedimentary model illustrating the relations between syntectonic deposition and tectonic activity, in the setting of the general evolution of foreland basin is summarized in Fig. 2.

At the basin scale (Fig. 2A), the subsiding foreland basin receives sediments from the growing orogen and in minor part from the craton margin. In the case of Taiwan, reworked nannoplankton and slate fragments found in the shallow-marine Plio-Pleistocene deposits show that sediments ran predominantly from the ENE indicating the location of the growing orogen (Covey, 1984). As the foreland basin is progressively filled in with the synorogenic deposits, the basin evolves progressively from dominant submarine to terrestrial sedimentation associated with upward coarsening of deposits. This general trend outlines the transition from underfilled to overfilled basin (Flemings and Jordan, 1989). In parallel, the abrupt increase of sedimentation/accumulation rates at a specific age is an argument for a large-scale tectonic event that would has induced the exhumation and denudation of the orogen. Although the large-scale lithology, for instance the coarsening of sediment with time, does not change significantly, the local thrust activity alters the deposition.

At the scale of a thrust-and-fold unit (Fig. 2B), local tectonic activity induces local subsidence due to thrust sheet loading, thus creating a foreland syncline in which syntectonic deposits accumulate. During initiation of individual thrusts, the basal depositional sequences of the submarine syntectonic strata are associated with local transgressive episodes subsequent to periods of relative quiescence characterized by regression and erosion or non-deposition in the proximal area. Moreover, when a thrust is activated the coarser sediments are trapped preferentially in the foreland syncline just ahead of the thrust. The resulting basal unconformity is thus better expressed in proximal domains and progressively diminishes toward the distal side. As the deformation propagates outward, successive local thrusting events (1–4 in Fig. 2) produce progressive syntectonic unconformities or onlaps (Riba, 1976; Anadon et al., 1986) onto the relative pre-growth strata deposited during former events.

In addition, numerous sedimentary markers can be used to constrain the local tectonic activity. For instance, when facies changes and syntectonic unconformities are associated with rotation of strata dips in the forelimb of anticline, olistolithes or slumping due to gravitational instabilities, the tectonic control on the sedimentation is unambiguously demonstrated

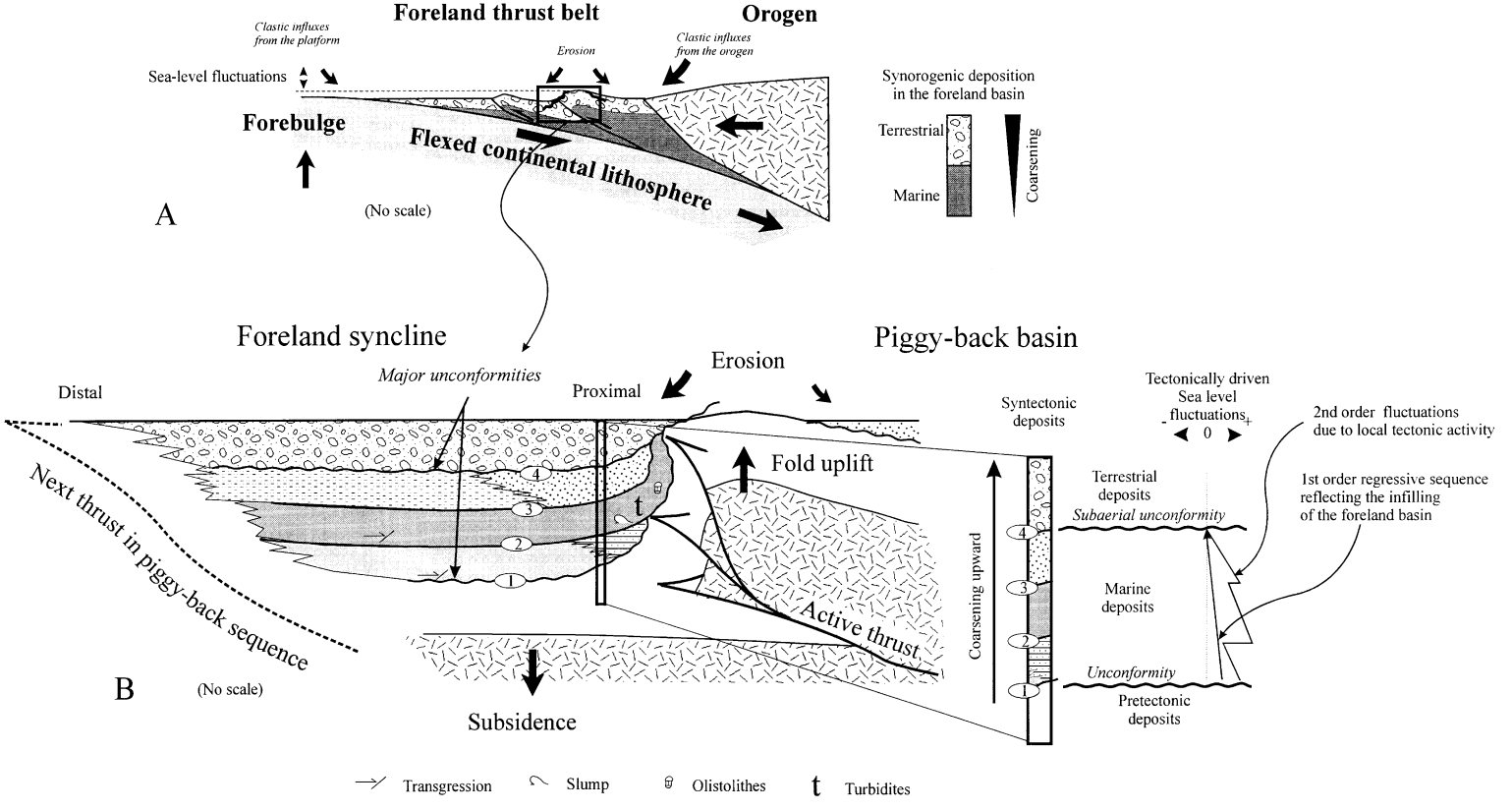

Fig. 2. Tectono-sedimentary record of foreland fold-and-thrust belt evolution: (A) at the basin-scale; and (B) at the scale of an individual thrust sheet.

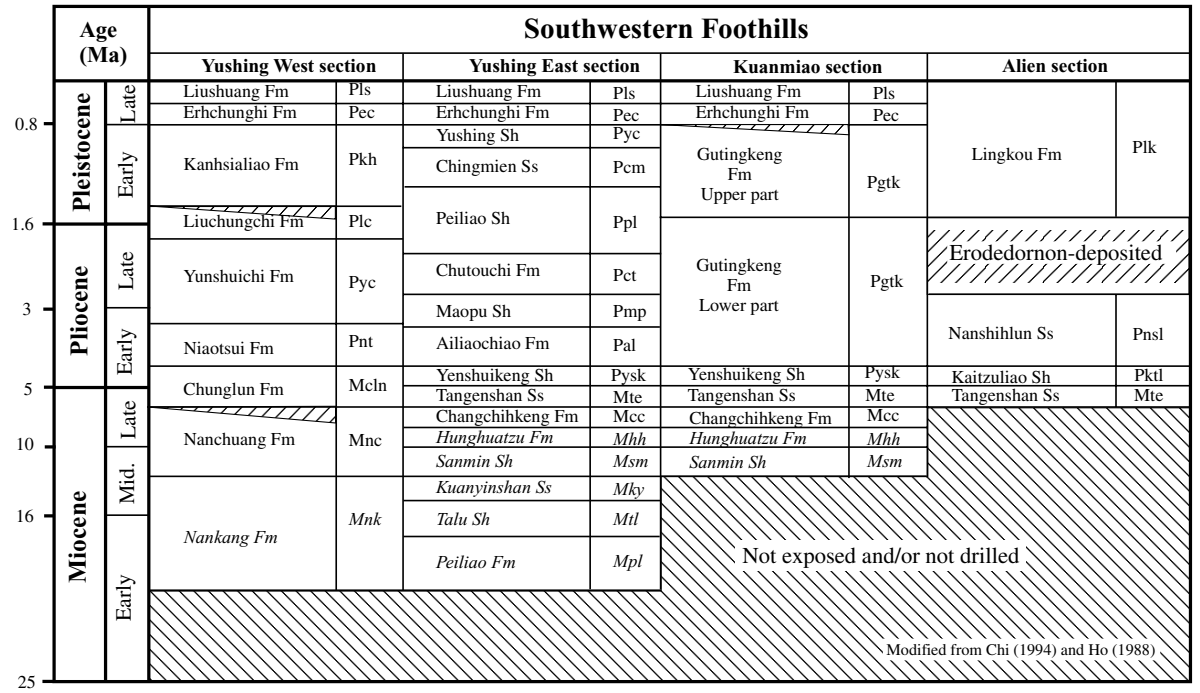

Fig. 3. Stratigraphy and time correlations between sedimentary formations discussed in the text and corresponding abbreviations. The units in italics are exposed north of the study area.

(Fig. 2B). Further, the recognition of turbidites in synorogenic deposits could also be used to constrain thrust activity provided that their local origin can be demonstrated, e.g. associated with previous syntectonic sedimentary indicators. Consequently, dating the syntectonic unconformities at minimum hiatus or other sedimentary indicators provides time constraints on thrusting events in the foreland thrust belt.

Summarizing, based on the analysis of synorogenic sedimentary sequences, we first attempt at distinguishing local and regional tectonic events, which have controlled the deposition in the southwestern thrust belt of Taiwan. Second, by dating initiation of thrusts and further reactivation induced by ongoing compressional deformation, we perform a sequential analysis of thrusting. Stratigraphic correlations between the different sedimentary formations that composed the studied areas are shown in Fig. 3. In the field, the tectono-sedimentary analysis has been carried out along three sections corresponding to sub-regions of the Southern Foothills (Figs. 1 and 4); the Yushing section, north of the CTFZ; the Kuanmiao section, within the CTFZ; the Alien section, near the southern extremity of the Foothills. The results of the tectono-sedimentary analysis are summarized for each investigated sections in a chronostratigraphic diagram (Fig. 5).

3.2.1. Yushing section

The sedimentary study of the Yushing province has been carried out within the five main thrust sheets that composed the tectonic pile. The oldest sediments are exposed in the innermost Chishan thrust sheet, limited to the east by the Chaochou fault bounding the Central Range; they consist of thick alternating shallow-marine to shallow bathyal shales and sandstones associated with numerous turbidites of the Late Miocene Changchihkeng formation (Figs. 4 and 5). These sediments were deposited on the Chinese continental margin after the rifting of the South China Sea and during the early uplift of the Peikang basement high (see previous section), in response to a preliminary contact between the Philippine Sea Plate (Luzon arc) and the Eurasian Plate (South China Sea). The upper Miocene Tangenshan formation (Figs. 4 and 5) locally overlies unconformably the Changchihkeng

formation and it is mainly represented by transgressive marine sandstones, fining upward, deposited in the shallow-marine environment as indicated, for example, by the numerous ripple cross-laminations and bioturbations. Just ahead of the Chishan thrust, the shallow-marine black shales of the Yenshuikeng formation are associated with bioclasts, calcareous olistolithes and locally contain fine-grained turbidites in which flute-casts indicate a transport from the NE (Figs. 4 and 5). These transgressive Early Pliocene shales and their related sedimentary patterns indicate the proximity of a topographic high to the east at the time of deposition, related to the initial activity of the Chishan thrust near 5 Ma (Figs. 4 and 5, index 1) and contemporaneous with the onset of the flexural subsidence. The overlying Ailiaochiao formation is composed of shallow-marine mudstones and fine-grained sandstones associated with strongly bioturbated facies and ripple marks. Further northwest, this formation is laterally correlated to the shallow-marine Niaotsui formation composed of fine to medium-grained sandstones interbedded with few thick dark mudstones associated with numerous fossils, ripples and hummocky cross-laminations (Eason, 1997) demonstrating that the basin deepened southwards. This lithofacies change shows either the relative quiescence of the thrust activity at that time or a rate of regional foreland subsidence greater than the fold uplift. West of the Pingchi thrust, the shallow-marine Maopu shales and Chutouchi formation consist, respectively, of dark gray shales and lenticular sandstones beds, separated by thick dark shales. Northwestwards, these deposits change laterally to mudstones and muddy sandstones of the Yunshuichi formation, exposed in front of the Lunhou thrust, in which dominant muddy facies, scarce sedimentary structures and intense bioturbations indicate slow deposition was in a low-energy environment corresponding to an offshore environment deeper than the underlying Niaotsui formation. Moreover, the occurrence of turbidites within the Maopu shales, nearby the present position of the Pingchi thrust might argue in favor of the initiation of this fault at 3.4 Ma (Figs. 4 and 5; index 2) and probably renewed thrusting along the Chishan thrust at the same time. This demonstrates that the distal part of the basin continued to subside while the inner part was deformed and uplifted. Upward, a syntectonic unconformity is observed between channelized and folded fine-grained sandstones of the upper Chutouchi formation and muddy dominant shallow-marine deposits of the Peiliao shales (Figs. 4 and 5; index 3). To the northwest, these latter are correlated with the Liuchungchi formation exposed in the area of the Lunhou thrust, which is dominated by dark mudstones and muddy sandstones. Complete or incomplete turbidites sequences are also found within the sandstones of this formation associated with few slumps and were interpreted as a submarine canyon system (Eason, 1997). The Liuchungchi was deposited on an unstable outer shelf and/or an upper slope. The upper Liuchungchi formation is unconformably overlain by the Kanhsialiao formation (Figs. 4 and 5). The unconformity is also observed westward beneath the Coastal Plain and offshore and is characterized by an irregular surface with slumps and channels. Since the Early Pleistocene (1.6 Ma), the deposition in the inner part of the thrust belt become fluvial and near shore as shown by the deposition of the Lingkou formation in inner part of the Kuanmiao and Alien sections (Figs. 4 and 5). At that time sedimentation rates increase to about 2 km/Ma (Chang and Chi, 1983) (Fig. 6). The rapid infilling of the basin and the high sediment influx could be interpreted as a result of the rapid denudation of the Central Range in the Mid-Pleistocene. Consequently, the high-energy deposition of the Liuchungchi can be regarded as the record of a regional tectonic event outlined by a regional transgression followed by a rapid progradation during relative quiescence. This type of large-scale sedimentary architecture agrees with predictions of the modeling of tectonically controlled sea-level fluctuations within foreland (Jordan and Flemings, 1991). Moreover, the deposition of the Liuchungchi formation was probably enhanced by the initiation of the Lunhou thrust near 2 Ma (Figs. 4 and 5, index 4). Eastward, the Peiliao shales were deposited in piggy-back position with respect to the Lunhou thrust sheet and have recorded a second motion of the Pingchi thrust as suggested by the unconformity at the base of the shales (Figs. 4 and 5, index 3). To the west of the Chutouchi thrust, the Yushing foreland syncline is filled with the Pleistocene Chingmien formation and the Yushing shales composed of mudstones with channels of sandstones, cross-bedded strata and numerous fossils that indicate a marine deltaic

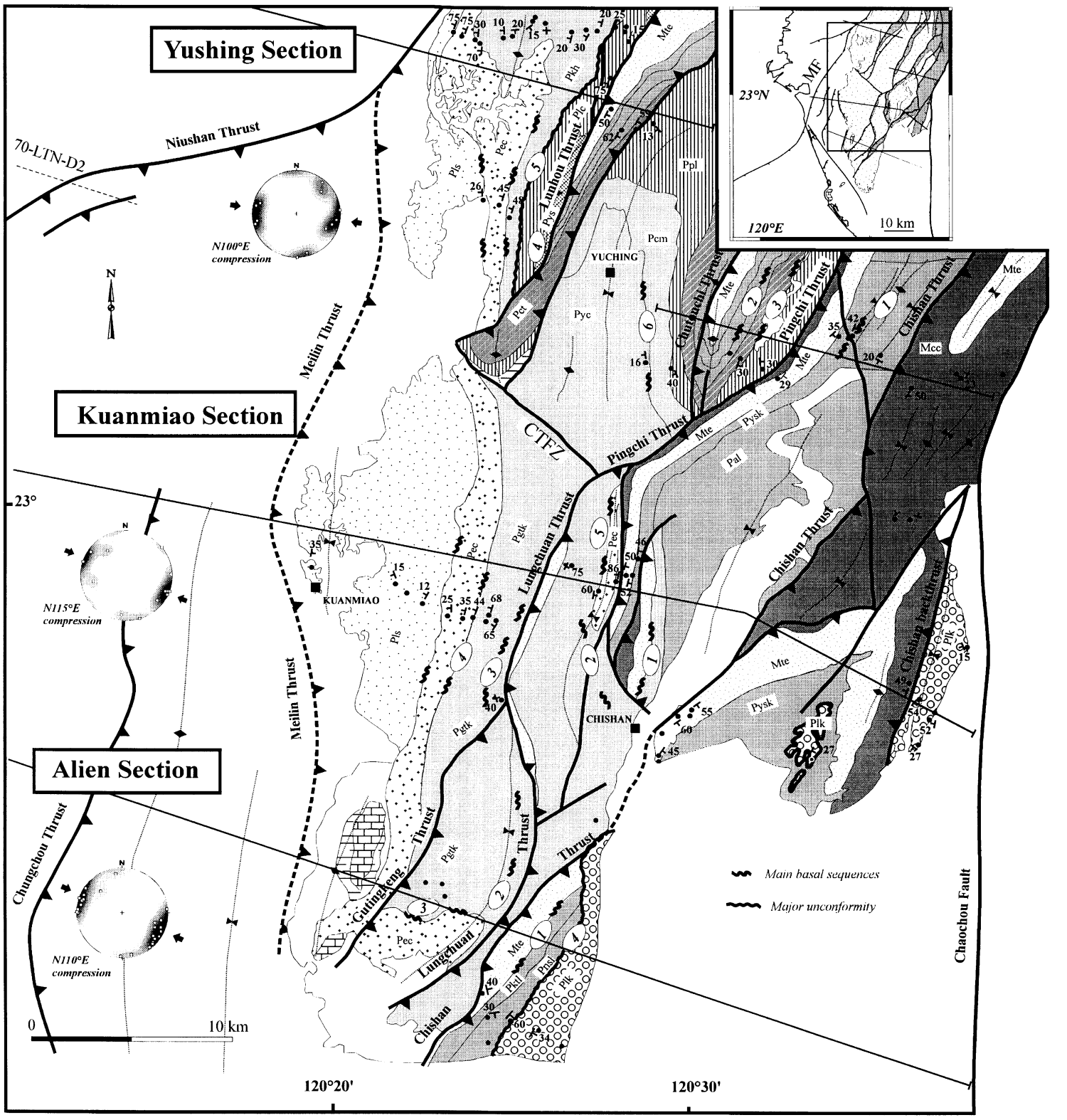

Fig. 4. Geological and structural map of the southwestern Foothills. Black dots correspond to main sites where sedimentary analysis was carried out. Major unconformities, basal sequences and numbered indexes refer to those shown in Fig. 5. For abbreviations refer to Fig. 3. (MF): Mountain front. The location of the Meilin thrust (dashed lines) outlines a topographic boundary between the Western Foothills and the Coastal Plain.

F. Mouthereau et al. / Tectonophysics 333 (2001) 293–322

pp. 301–302

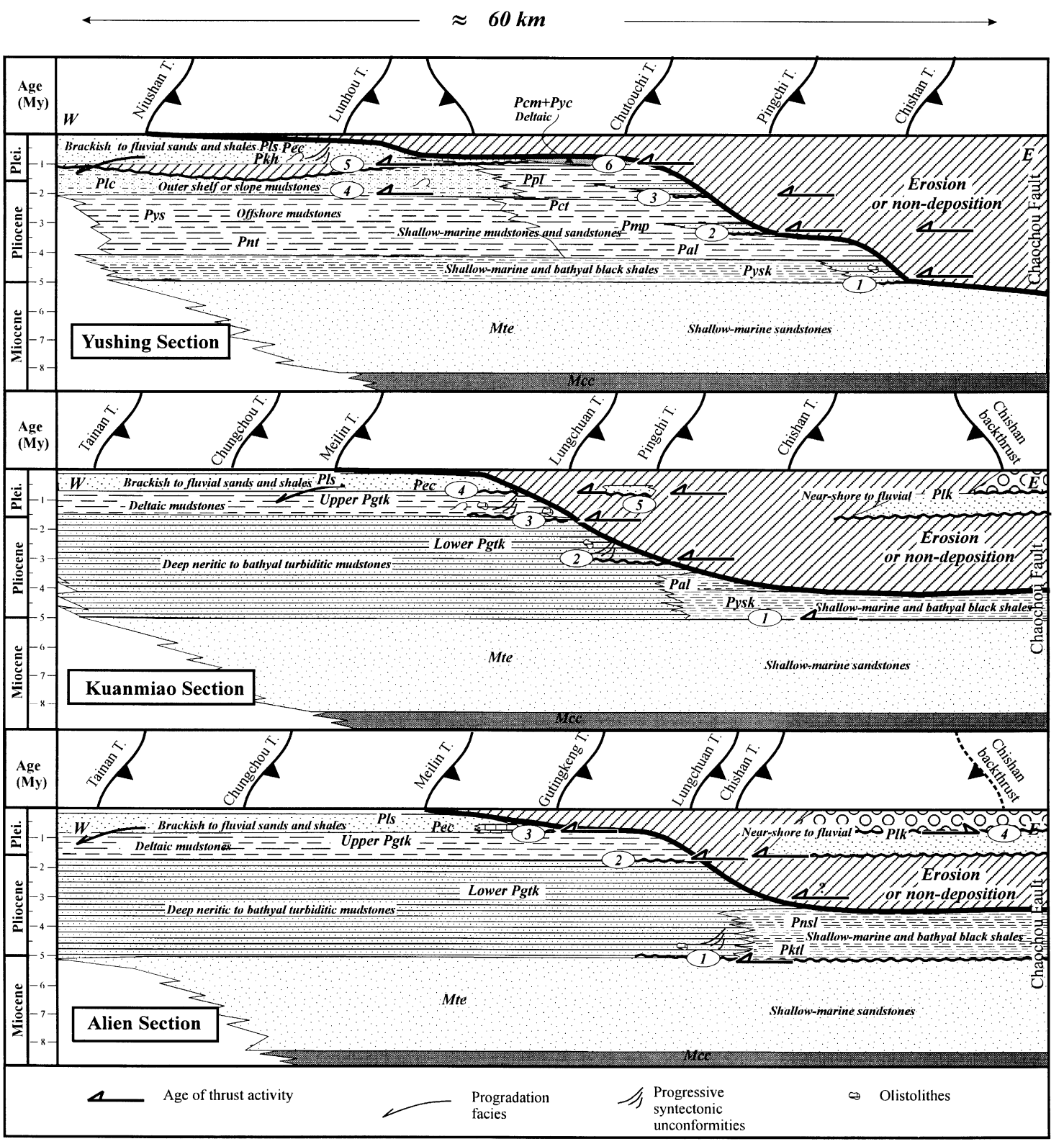

Fig. 5. Stratigraphic diagram showing tectono-sedimentary evolution though time in the three investigated areas of the southwestern Foothills. Lateral lithofacies change and sedimentary indicators used in this study are presented (also refer to Fig. 2). Thrust activities are indicated by arrows and indexes (also refer to Fig. 4). Thrusting mainly occurred in-sequence with progressive uplift and erosion of older thrust units.

environment. This formation is correlated westward to the Kanhsialiao formation, which is transgressive onto the Liuchungchi formation. The Kanhsialiao formation consists mainly of mudstones with local occurrence of sandy turbidite beds and was deposited in lower slope environment. The deposition of the Kanhsialiao formation might be correlated with a large-scale tectonic event at 1 Ma coeval with the deposition of the upper Lingkou conglomerate in the inner Foothills. The activity of the Lunhou thrust controls the deposition of these turbidites and locally enhanced the regional subsidence (Figs. 4 and 5, index 5). The Yushing/Chingmien formation was deposited in a piggy-back basin limited to the west by the Lunhou thrust and control to the east by the initiation of the out-of-sequence Chutouchi thrust at nearly 1 Ma (Figs. 4 and 5, index 6). Located in the frontal syncline of the Lunhou thrust, the Late Pleistocene prograding sequence (since 1 Ma) nearly 4 km thick shows the highest accumulation rates in the Western Foothills, about 3 km/Ma (Chang and Chi, 1983) (Fig. 6).

The Kanhsialiao formation is unconformably overlain by the Erhchungchi formation, which is composed of interbedded shallow-marine sandstones and mudstones. Some coarse-grained turbidite sequences are found (Eason, 1997) and erosional and channelized surfaces are also observed. The scarcity of bioturbation and predominance of sedimentary structures exhibit the rapid infilling and the high-energy deposition on an unstable deltaic environment. The marine erosive surface and transgression are interpreted as resulting from the reactivation of the Lunhou thrust near 0.8 Ma. The overlying Liushuang formation consists of brackish to fluvial mudstones and sandstones as attested by the numerous near shore fossils such as mammalia, amphibia, drift wood and fishes in the lower part and the numerous fluvial sedimentary structures in the upper part (Eason, 1997). The deposition of the Liushuang formation can also be interpreted in response to the activity of the Lunhou thrust near 0.4–0.5 Ma. In the meantime, erosion occurs in most areas of the Foothills. Both Erhchungchi and Liushuang formations show the rapid westward progradation of the facies associated with progressive unconformities. In addition, the syntectonic strata have been progressively rotated in the fold hinge in the vicinity of the Lunhou thrust (Fig. 4). All these observations demonstrate that the deposition of the most recent syntectonic deposits have been mainly controlled by the motion of the Lunhou thrust with the general tendency for the foreland basin to be overfilled. The outermost Niushan thrust separates the Coastal Plain and its quaternary alluvial deposits from the Western Foothills (Figs. 3 and 4). A seismic reflection profile provides further constraints on the age of the initiation of the Niushan thrust (see discussion on cross-sections) which might be firstly activated after the deposition of the Liushuang, not before 0.4–0.5 Ma.

3.2.2. Kuanmiao section

Most of western thrust sheets recognized in the previous Yushing section is interrupted across the surface trace of the CTFZ except the inner Chishan and Pingchi thrust units, which extend southwards (Figs. 4 and 5). This fact argues in favor of the late reactivation of these thrusts, demonstrating that the ongoing deformation occurred in the frontal portion of the thrust belt as well as at the rear. To the eastern end of the Kuanmiao section, the Chishan thrust sheet is associated with the development of a pop-up structure. The sands belonging to the basal Lingkou formation are found within the Chishan pop-up and unconformably overlie the Yenshuikeng shales. These deposits correspond to near-shore to fluvial meandering environment with some fossils wood, and rather indicate a low energy transport (Figs. 4 and 5). The hiatus in between the Yenshuikeng and Lingkou formations is due to the continuous erosion and non-deposition at the back of the growing Chishan thrust and pop-up. Consequently, dating the initiation of the backthrust is ambiguous, even though it occurred after 4 Ma as indicated by the upper unconformity of the Yenshuikeng formation. In order to solve this problem and determine more accurately the episode of thrusting related to the formation of the Chishan backthrust, complementary observations are necessary in more distal localities because hiatus diminishes basinwards. Wedged between the east-verging thrust and the Chaochou fault bounding the Central Range, a thick series of coarse-grained and cobbly continental deposits of fluvial origin is exposed (Figs. 4 and 5). The corresponding Lingkou conglomerates are folded and arranged as a syncline. This syncline corresponds to a gravity low (Hsieh,

1970), indicating a thick series of low-density sediments. The deposition of the upper Lingkou conglomerates corresponds to a braided river environment and reflects a significant increase of fluvial transport energy, consistent with the important acceleration of uplift of the mountain range near 1 Ma (Lee, 1977). The deposition of the Early Pliocene Yenshuikeng and Ailiaochiao formations can be interpreted in the same way as for the Yushing section and outlines the first motion of the Chishan thrust in the Early Pliocene near 5 Ma (Figs. 4 and 5, index 1). West of the Pingchi thrust, in the Lungchuan thrust sheet (Figs. 4 and 5), the syntectonic deposits are dominated by the thick Plio-Pleistocene mudstones of the Lower Gutingkeng formation (up to 2–3 km thick), in which the basal part is correlated with the shelf deposits of the Yenshuikeng and Ailiaochiao formations. Only the older part of the Gutingkeng is observed in the Lungchuan thrust sheet. According to the benthic foraminiferal assemblages (Oinomikado, 1955) and sedimentary facies analysis (Covey, 1986) of the constitutive mudstones, the Gutingkeng formation corresponds to moderately deep offshore marine strata (Horng and Shea, 1994), which confirms the southward deepening of the basin. West of the Pingchi thrust, the lower Gutingkeng sediments are usually found in association with turbidites and olistolithes arguing in favor of a slope environment during the deposition of the mudstones (Figs. 4 and 5) in a subsiding foreland syncline mainly induced by regional flexural subsidence and enhanced by the load of the Pingchi thrust. Based on correlation between nannofossils and planktonic foraminifera, Horng and Shea (1994) have demonstrated the occurrence, in this area, of an intraformational unconformity dated in the interval 2.9–1.9. These results suggest that the Pingchi thrust (Figs. 4 and 5, index 2) was initiated during the Middle Pliocene at about 3 Ma such as in its northern branch. To the west, the bedding of the upper part of the Gutingkeng becomes steeper in the vicinity of the Lungchuan thrust and is even overturned in numerous places (Fig. 4). This suggests that rotation occurred during deposition in response to the activity of the Lungchuan thrust. The uppermost part of the Gutingkeng formation corresponds to a marine deltaic environment (Covey, 1984) and could be correlated with the Yushing and Kanhsialiao formations found northward. In addition, in the vicinity of the Lungchuan thrust, occurrence of olistolithes and slumps associated with the Gutingkeng formation dates the first motion of the Lungchuan thrust near the Pliocene–Pleistocene boundary at 1.6 Ma (Figs. 4 and 5, index 3). In the central part of the frontal syncline, the Erhchungchi formation unconformably overlies the Gutingkeng formation demonstrating that the Lungchuan thrust was still secondarily active at that time, near 0.8 Ma (Figs. 4 and 5, index 4). Moreover, in front of the Pingchi thrust sheet the Erhchungchi formation overlies unconformably the lower Gutingkeng thus defining an important hiatus. This may indicate that the Pingchi thrust was reactivated near 0.8 Ma (Figs. 4 and 5, index 5) and creates conditions for the transgression of the Erhchungchi formation onto older units. We propose to connect this unconformity with the major unconformity between the Kanhsialiao and the Liuchungchi formations observed northward. Upward in the sedimentary sequences, the deposition of fluvial and lagoonal sands of the Liushuang at 0.4–0.5 Ma formation marks also a sequence boundary corresponding to the development of a prograding syntectonic wedge in relation with continuous activity of the Lungchuan through the Pleistocene.

3.2.3. Alien section

The main structural difference with regard to the other sections is the limited number of thrust units. We first distinguish one major thrust sheet that corresponds to the easternmost Chishan unit bounded to the west by the Chishan thrust and buried to the east beneath the deposits of the Pingtung depression. In the Chishan thrust sheet, the Miocene sandstones of the Tangenshan formation were deposited in the upper shelf (Figs. 4 and 5). To the east of the Chishan thrust, the shallow marine sandy shales and sandstones of the Kaitzuliao formation unconformably overlie the Tangenshan sandstones and were deposited in a piggy-back basin located on top of the growing Chishan thrust. The occurrence of turbidites within this formation argues in favor of a local gravitational instabilities related to the initiation of the Chishan thrust in the Early Pliocene at 5 Ma (Figs. 4 and 5, index 1). These deposits are correlated west of the Chishan thrust with the thick mudstones of the Gutingkeng formation, which were deposited in the subsiding syncline ahead of the Chishan thrust.

According to the model of Fig. 2, both types of facies confirm the age of the initiation of the Chishan thrust sheet near 5 Ma. The overlying Nanshihlun formation is composed of storm-dominated shallow marine sediments (Covey, 1984). Both Pliocene Kaitzuliao and Nanshihlun formations thicken toward the Pingtung plain as revealed by the PTG-1 well (Hsieh, 1970); this confirms that they were deposited in piggy-back basin at the front of the Central Range. Such as in the Kuanmiao section, the marine Pliocene sedimentation is followed by the deposition of the Lingkou sands and conglomerates of fluvial origin. These sediments unconformably overlie the Lower Gutingkeng (southward), Nanshihlun, Kaitzuliao and the Tangenshan formations and the related angular unconformity is well outlined in the field (Fig. 4). This major unconformity indicates that the Chishan piggy-back basin was drastically uplifted and tilted after the deposition of a lower part of the Gutingkeng formation suggesting the reactivation of the Chishan thrust after 3 Ma coeval with the Pingchi thrust initiation to the north and also probably near 1.6 Ma as indicated by the deposition of the upper Gutingkeng in the foreland, coeval with the initiation of the Lungchuan thrust, and the deposition of the basal Lingkou formation in the piggy-back basin. Then the fluvial sediments of the upper Lingkou conglomerates were deposited and tilted indicating a recent thrusting event during the last 0.8 Ma (after the deposition of the upper Lingkou conglomerates). This event may be related to the initiation of the Chishan backthrust thus outlining the Chishan pop-up structure. The duration of this catastrophic sedimentation through the Pleistocene indicates the continuous accumulation in the subsiding Pingtung depression. The extension of the Lingkou formation is presently limited to the east by the Central Range and to the west by the Chishan thrust sheet, which have probably acted as a barrier for the sedimentary supply from the unroofed Central Range. Consequently, we propose to connect the deposition of the coarse-grained Lingkou formation with a major kinematics event in relation with the exhumation and denudation of the Central Range. This remarkable tectonic episode occurred out-of-sequence with respect to the evolution of the Foothills, after the initiation of the Chishan thrust located westward. As in the Kuanmiao section, the deposition of the upper part of the Gutingkeng formation is an indicator of the first movement along the Lungchuan thrust (Figs. 4 and 5, index 2) near 1.6 Ma. West of the Gutingkeng thrust unit, the Takangshan reefal limestones have been interpreted as the result of reef building on top of growing anticline (e.g. Lacombe et al., 1997, 1999). The relative topographic high creates favorable paleoecological conditions for the growth of reefal limestones by isolating them from the clastic influxes from the orogen. These limestones are dated at 0.7–0.5 Ma (Erhchungchi formation) and may be correlated with the initiation of the Meilin thrust contemporaneous with folding (Figs. 4 and 5, index 3). Furthermore, their deposition may also be enhanced by a transgressive episode induced by the initiation of the Gutingkeng thrust near 0.8 Ma.

3.2.4. From local-scale to basin-scale tectono-sedimentary evolution

Based on estimates of ages of thrust initiation and potential reactivation along the three sections coupled with the general sedimentary evolution of the southwestern foreland basin it is possible to draw a qualitative scheme of first and second-order tectonic events. The results are synthesized in Fig. 6.

Three major tectonic stages or "pulses" (A, B and C in Fig. 6A and B) may be recognized within the southwestern Foothills, which are correlated with local thrusting events.

The first stage (A) just follows the initial flexure of the basement and continues throughout the Pliocene (Fig. 6A). This initial stage of the collision is associated with limited thrust activity outlined by the initiation of the Chishan thrust near 5 Ma and the Pingchi thrust near 3–3.4 Ma and reactivation of Chishan thrust at the same time. The weak tectonic activity during this initial episode is correlated with dominant shallow-marine deposition, continuous deepening of the basin with low subsidence rates and low sedimentation rates $< \sim 1$ km/Ma (Fig. 6B). Local and large-scale tectono-sedimentary data indicate an initial submarine accretionary stage during which the foreland basin is mostly underfilled.

The second stage (B) occurs in Late Pliocene–Early Pleistocene (2–1.6 Ma) and corresponds to a transitional stage toward a higher energy depositional system within the basin, which is progressively affected by increasing thrust propagation and increasing erosion of the orogen. This "intermediate"

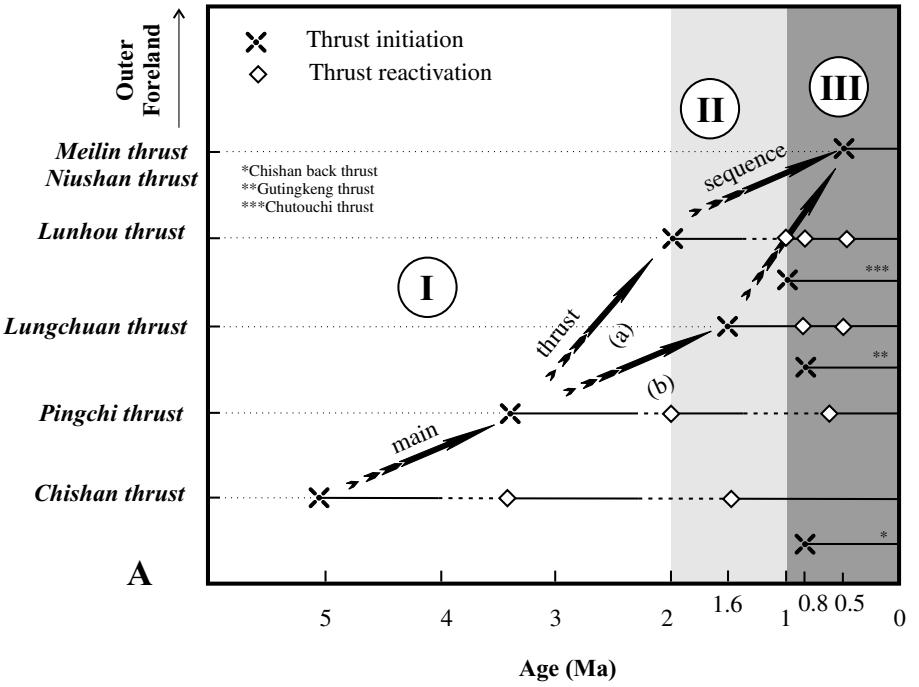
Outer Foreland
Thrust initiation
Thrust reactivation
I
II
III
Meilin thrust
Niushan thrust
*Chishan back thrust
**Gutingkeng thrust
***Chutouchi thrust
Lunhou thrust
Lungchuan thrust
Pingchi thrust
Chishan thrust
sequence
thrust
(a)
(b)
main
***
**
*
A
5
4
3
2
1.6
1
0.8 0.5
0
Age (Ma)

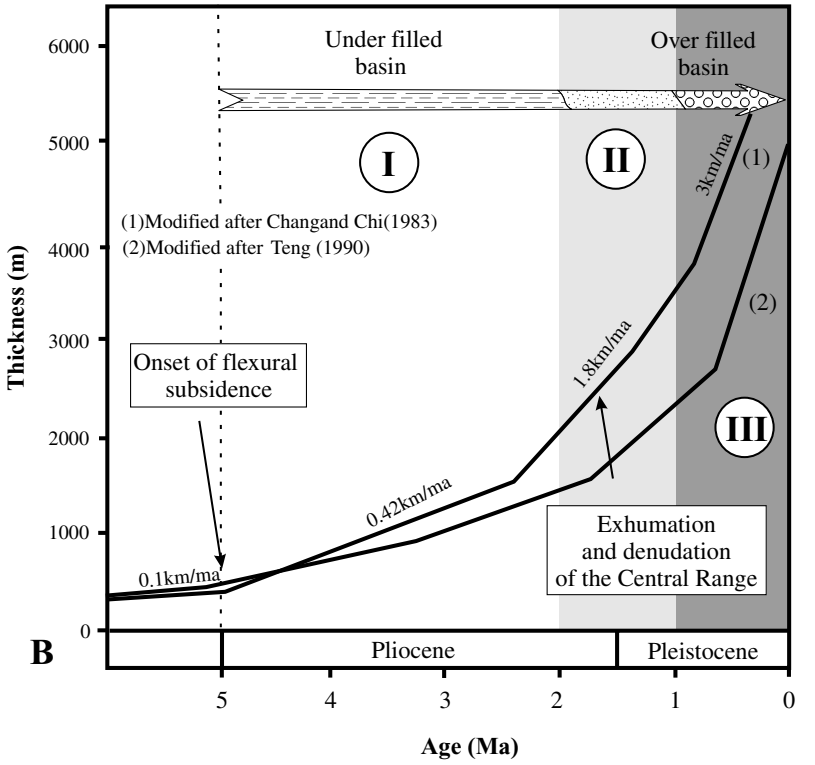
Under filled basin
Over filled basin
I
II
III
(1)Modified after Changand Chi(1983)
(2)Modified after Teng (1990)
Onset of flexural subsidence
3km/ma
(1)
(2)
1.8km/ma
0.42km/ma
0.1km/ma
Exhumation and denudation of the Central Range
Thickness (m)
6000
5000
4000
3000
2000
1000
0
B
Pliocene
Pleistocene
5
4
3
2
1
0
Age (Ma)

collision stage (in between 2 and 1 Ma on average) is marked by the initiation of the Lunhou and Lungchuan thrusts and renewed thrusting of the Pingchi and Chishan thrusts at 2 and 1.6 Ma (Fig. 6A). At that time, an increase in accumulation rates from ~0.5 to ~2 km/Ma occurs and may be related to the rapid exhumation and denudation of the Central Range (Fig. 6B). This is also correlated with the increase of flexural subsidence outlined by a regional transgression followed by rapid progradation. This stage outlines the tendency for the foreland basin to be overfilled.

The last major tectonic event (C) occurs in the Middle Pleistocene near 0.8–1 Ma and leads to the building of the present-day structural and sedimentary patterns of the southwestern Foothills. At that time, most of the thrusts are active or reactivated and out-of-sequence thrusting (Chutouchi thrust) and back-thrusting occurs (Chishan backthrust) (Fig. 6A) indicating that the shortening increases without forming new thrusts at the front. High accumulation of syntectonic deposits occurred, as indicated by the highest sedimentation rate of the Taiwan Foothills attaining 3 km/Ma (Fig. 6B), and were preferentially deposited in the outermost part of the Foothills and in the Coastal Plain. This may prevent the westward propagation of the thrust wedge. At that time, the syntectonic deposition evolves progressively to brackish and fluvial facies demonstrating that the southwestern foreland thrust belt is progressively exposed and turn into the present-day subaerial foreland thrust belt.

4. Restoration of cross-sections, structural styles and estimation of amount of shortening

In the studied area, the subsurface data used to constrain the balanced cross-sections are mostly based on the available wells drilled within the Coastal Plain and Western Foothills and have been completed by field measurements. It should be pointed out that the subsurface geologic interpretation of ancient seismic reflection profiles established by the Chinese Petroleum Corporation remains ambiguous because of the poor resolution in this area (personal communication). Furthermore, these seismic lines are usually restricted to the first thrust units and hence are just of local interest. Consequently this work must be seen as a preliminary study, which should be improved by further subsurface structural investigations.

The cross-sections presented in this work have been balanced by using the computer-aided LOCACE® software (Moretti and Larrere, 1989). The tectono-sedimentary analysis has provided additional control on the deformation history prior to balancing and restoration of the cross-sections. All the sections have been restored backward into an initial stage of compressional deformation with respect to a reference level that corresponds to the top of pre-collisional strata, taken as the top of the upper Miocene Tangenshan sandstones.

Some basic assumptions are required before balancing. First, the sections must be constructed parallel to the transport direction. This point is solved by the observation of average trends of regional folding and major faults and also by transfer faults. We determine from the geological map of the Chinese Petroleum Corporation (Fig. 4) that the average transport direction is N100°–110°E on average, perpendicular to regional structures and trending slightly oblique to the CTFZ. Second, the deformation must be strictly confined to the plane of the section (plane strain), which is reasonable regarding the fact that no important lateral motion occurred along the major thrusts and within thrust sheets. In addition, statistical analysis of compressional trends from paleostress reconstructions has been carried out in the studied areas in order to constrain the mean direction of shortening that prevailed during the emplacement of thrust systems.

Fig. 6. Correlation between regional and local tectonic evolutions in the southwestern foreland thrust belt during the Plio-Pleistocene collision. (A) Timing of local thrust activity. Arrows indicate the main sequence of thrusting (in-sequence) for (a) Yushing section and (b) Kuanmiao–Alien section. (B) Curves of regional sedimentation rates. The good correlation between both local and large-scale evolutions demonstrates that local tectono-sedimentary record reflects major trends of basin-scale evolution. Three major stages are identified in the investigated areas: (I) initial submarine accretionary prism stage (underfilled foreland basin); (II) "intermediate" stage; and (III) subaerial foreland thrust belt stage (overfilled foreland basin) (see text for detailed explanations).

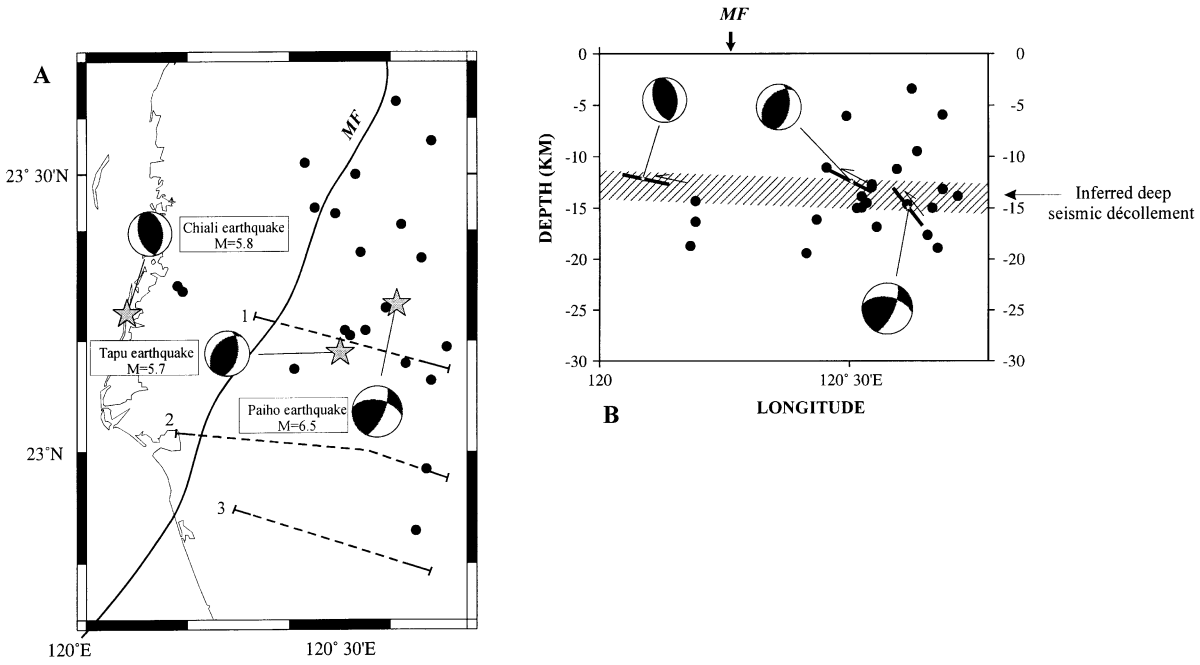

Fig. 7. Seismological evidence of a 12–15 km deep décollement beneath the Western Foothills and Coastal Plain of southern Taiwan. (A) Map location of low-to-moderate ($3 < M < 5$) earthquakes (black dots) used by Rau and Wu (1998) to calculate focal mechanisms. Stars and fault plane solutions correspond to the three major earthquakes ($M > 5$) that occurred since the last 40 years. (B) Depth distribution of seismicity on cross-section of the Southernwestern Foothills and Coastal Plain. Location of studied geological cross-sections is shown (1, 2 and 3). (MF): Mountain front.

4.1. Shallow and deep-seated décollement levels

Prior to construct retrodeformable cross-sections, we discuss the location of the potential décollement levels based on lithology and seismicity constraints.

The oldest formations exposed in the southwestern Foothills are represented by a thick alternating shallow-marine to shallow bathyal shales and sandstones of the Changchihkeng formation (Figs. 3 and 4). Based on field arguments and exploration wells, Ho (1988) indicates that the total thickness of this formation may reach 1600 m or more. Furthermore, North of the study area, the Changchihkeng formation overlies the older Hunghuatzu formation and Sanmin shales (Fig. 3). These Late Miocene formations consist of a thick stratigraphic assemblage of 2000–3000 m in which shales represent the main part. Moreover, the geological mapping reveals that the Changchihkeng formation is mainly exposed in the hangingwall of the major thrusts and strikes parallel to the Chishan and Pingchi thrusts over a large distance (Fig. 4). These arguments lead to interpret this formation and further the overall Late Miocene assemblage (Changchihkeng, Hunghuatzu and Sanmin formations), as a basal décollement level for the Neogene cover. Moreover, the geological map of Chinese Petroleum Corporation (1989) completed by our field observations indicate that these Miocene shales are intensely folded as shown by the numerous disharmonic folds of few kilometers of extension to one meter to tens of meters amplitude. Further structural evidences indicate that the mechanism of deformation is mostly represented by superimposed flexural flow and flexural slip mechanisms. Consequently, the Late Miocene strata have probably behaved as a thick ductile layer under the Plio-Pleistocene compressional deformation. Based on the thickness of neogene strata the average depth of the basal décollement is 6–8 km. The occurrence of such ductile level allows the upper Neogene strata to be detached and deformed independently with respect to the underlying pre-Miocene strata, which are

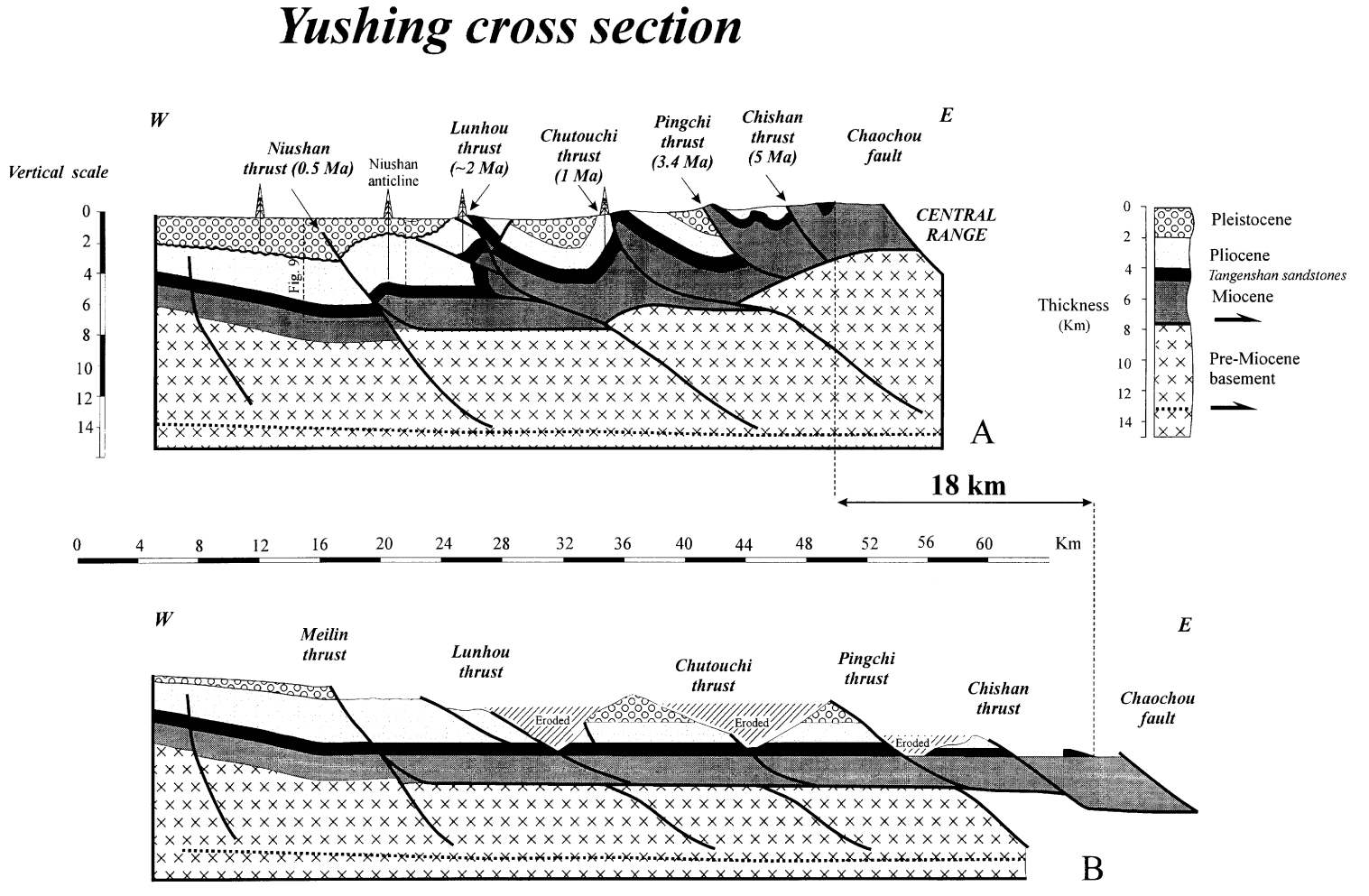

Fig. 8. Yushing balanced cross-section (A) and restored cross-section (B). The frame in dashed lines corresponds to the projection of the seismic reflection profile shown in Fig. 9.

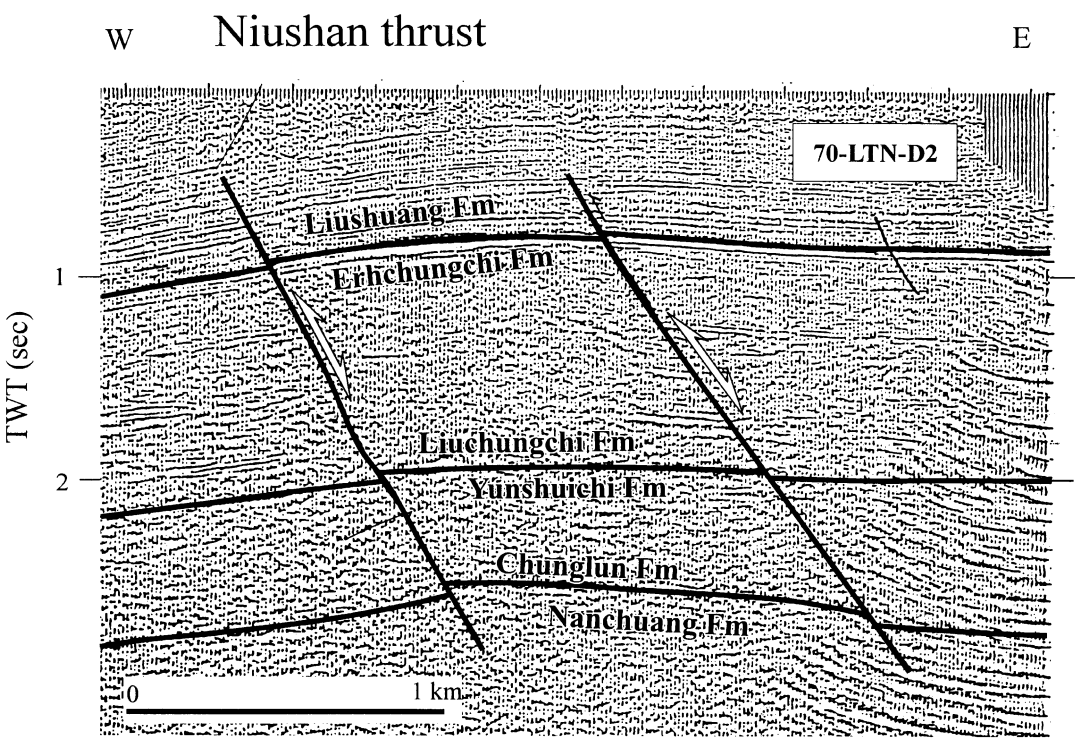

Fig. 9. Seismic reflection profile characterizing the Niushan thrust beneath the Coastal Plain (after Hu and Sheen, 1989; see location in Fig. 3). The steeply dipping attitude of thrust faults and the locally preserved normal offset support structural inversion beneath the Niushan anticline.

considered as a good proxy for the basement rocks. Because of its particular behavior, this layer has been restored by using a "free" method usually applied to restore salt levels.

By using this method, local ductile thickening beneath anticlines might be simulated and thus provide an alternative hypothesis with regard to other hypotheses such as roof stacked duplexes. In contrast, upper (Plio-Pleistocene) and lower (pre-Neogene) strata have been restored by using classical flexural slip/parallel slip method. An other example of such type of restoration can be found in Colletta et al. (1999) who proposed for the sub-Andean ranges of southern Bolivia that interbedded shales within the cover behave as an intermediate detachment which are thickened in fold hinges.

The pre-collisional history of the southern foreland thrust belt is shown by the abrupt changes in thickness and deformation style of Miocene deposits in the vicinity of major thrusts. Furthermore, the involvement of the pre-Miocene strata in the shortening, even in the frontal part of the section, has been already proposed in this area (Chang et al., 1996; Hung et al., 1999; Mouthereau et al., 1999, 2001). The involvement of pre-Miocene basement in the deformation leads to discuss the occurrence of a deeper décollement beneath the southwestern Foothills. Regarding the seismicity, the depth of such décollement could be proposed. North (Yushing section) and within the CTFZ (Kuanmiao section), the seismicity related to the collisional shortening is diffuse and ranges in depth from 0 to 20 km; focal mechanisms of low to moderate earthquakes ($3 < M < 5$) calculated after Rau and Wu (1998) for the 1991–1994 period are nevertheless concentrated on average to depth of 12–15 km on average (Fig. 7). Inversion reveals that all of these focal mechanisms are compatible with a N97°E compression (Lacombe et al., 2000).

In addition, the study of major earthquakes in southern Foothills provides further information on the depth and mechanisms of the potential deep décollement. The recent Chiayi earthquake of 25

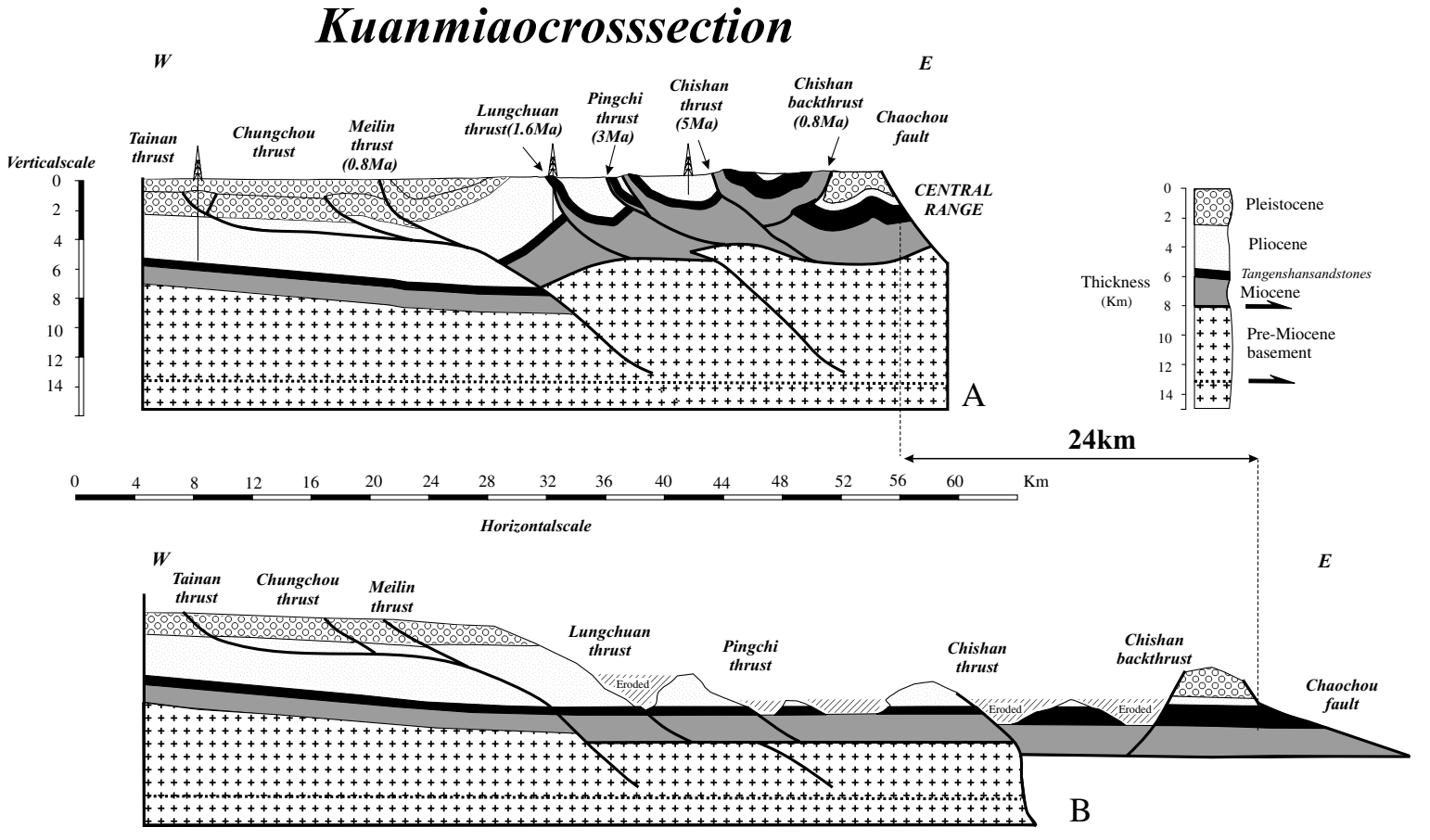

Fig. 10. Kuanmiao balanced cross-section (A) and restored cross-section (B).

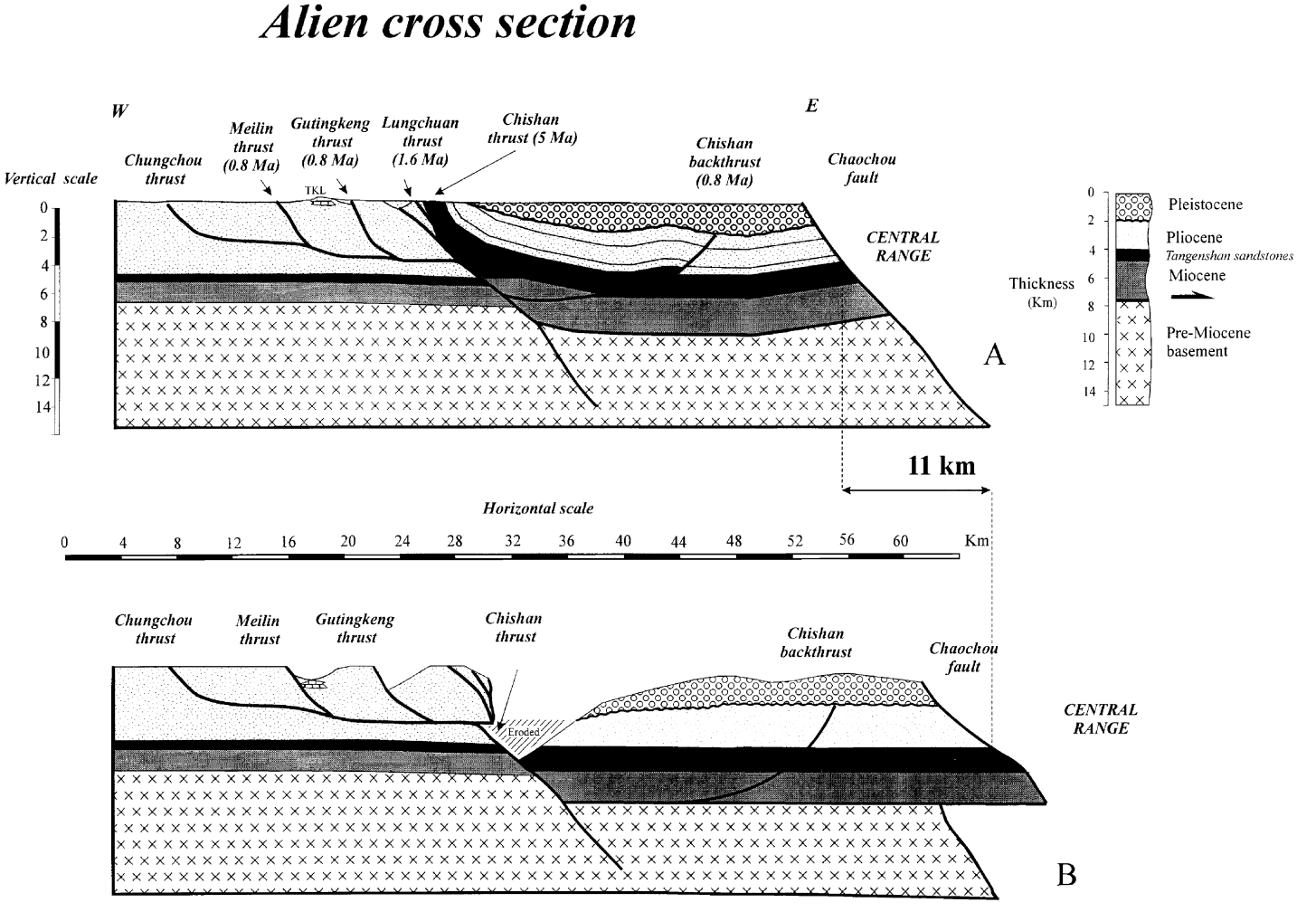

Fig. 11. Alien balanced cross-section (A) and restored cross-section (B).

September 1999 Mw = 6.4) occurred few days after the destructive Chichi earthquake of 21 September 1999 (Mw = 7.6) (Ma et al., 1999). The hypocenter of the earthquake is located to depth of 12.1 km, 10 km to the north of the Yuching section, and shows a compressive mechanism (data from Central Weather Bureau). The Chiali earthquake occurred on 12 March 1991 (Ml = 5.7 to the west of the Yushing section to depth of 12.26 km (Ma and Chen, 1999) and indicates a compressive mechanism (Fig. 7). Other large earthquakes such as Tapu earthquake of the 15 December 1995 (Huang et al., 1996) and Paiho earthquake of the 18 January 1964 (Chang and Yeh, 1981) near Yushing section indicate that active reverse faults exist to depth greater than 10 km. Combining these results argue in favor of an upper crustal seismic décollement located to depth of 12–15 km on average (Fig. 7). In contrast, the upper décollement (6–8 km) deduced from structural arguments is probably less active or even aseismic, which is not surprising regarding its ductile behavior.

Therefore, we must consider two superimposed types of deformation in our cross-sections; one involves cover strata and represents the classical thin-skinned tectonics, which was extensively described in Taiwan (Suppe 1976; Suppe and Namson, 1979, 1980, 1981; Namson, 1981) and another involves deeper units and basement in the deformation and corresponds to thick-skinned tectonics. Such a combination of shallow and deep-décollement tectonics has been also proposed for the frontal thrust units of the Taiwan Foothills (Mouthereau et al., 1999, 2001).

4.2. Yushing section

The Yushing section (Fig. 8) is located north of the CTFZ and is subdivided in two sections in order to take into account the available wells and structural data. Based on statistic analysis of paleostresses we determine an average regional N100°E shortening in the studied area (Fig. 4) subparallel to the regional N110°E transport direction deduced from trends of large-scale thrusts and folds. Additional minor compressive directions are also observed (N50°E and N160°E) representing second-order effects due to local kinematic rearrangement.

The westernmost part of the section is constrained by seismic reflection data (Hsiao, 1974; Hu and Sheen, 1989) up to 6 km depth. Other subsurface constraints are given by available wells explored by the Chinese Petroleum Corporation.

As suggested by the seismic profile 70-LTN-D2 located in the Coastal Plain (Fig. 9), the frontal Niushan thrust may be interpreted as resulting from the structural inversion of an inherited normal fault of the continental margin and subsequent thrusting above the lower Miocene décollement level (Fig. 8). This leads to another interpretation of the Niushan anticline that greatly differs from previous structural studies based on thin-skinned tectonics hypothesis (Suppe, 1980; Hung et al., 1999). To the west, in the Coastal Plain, we mostly found normal faults (Fig. 8), which are locally slightly reactivated near the southern edge of the Peikang high (Mouthereau et al., 1999, 2001).

The structural style of the Yushing section results from superimposed shallow and deep-décollement tectonics. The upper cover strata are shortened above a shallow-décollement located at the base of the Miocene shales. Below this upper décollement, the pre-Neogene strata and the basement were involved in the compression and were deformed independently by roofed imbricate basement thrusts detached above a deep-seated décollement. The geometric relationships between both structural systems and especially the folding of the upper décollement imply that the deformation of the upper units was secondarily controlled by late basement-involved tectonics. This type of evolution showing the influence of late deep-seated deformation onto shallow structure has been further proposed by Roure et al. (1990).

The restored section shows that basement thrusts are reactivated inherited extensional features of the stretched Chinese margin. For instance, the Chishan thrust at the rear of the tectonic wedge results from the inversion of an inherited normal fault as shown by thickness variations of Miocene deposits across the fault.

By considering the reference line at the base of the Pliocene strata (top of Miocene Tangenshan sandstones), we estimate an amount of shortening of nearly 18 km in the Plio-Pleistocene cover strata.

4.3. Kuanmiao section

The Kuanmiao section (Fig. 10) is located at the latitude of Tainan city within the Chishan Transfer Fault Zone. Most of thrust sheets are oriented

N20°E parallel to the general trends of the mountain belt. Locally the Pingchi thrust turns and strikes almost N–S close to the CTFZ (Fig. 4). This change in trend suggests that transfer faulting controls the kinematics of this area. An average regional N115°E shortening (Fig. 4) nearly parallel to the regional transport direction is determined. Additional minor compressive directions are also observed (N50°E and N160°E).

Such as in the Yushing section the decoupled cover and underlying basement sheets deformed nearly independently. The innermost Chishan thrust is continuous toward the south across the CTFZ and corresponds, as shown in the Yushing section, to an inverted normal fault. This major fault is associated at the rear of the thrust wedge with a backthrust and forms a large-scale pop-up structure.

The accommodation of shortening in the western part of the Kuanmiao section and the propagation of deformation were probably controlled by the deposition, in the foreland, of the thick pile of syntectonic sediments (5 km). Accumulation of syntectonic strata in the frontal part of the thrust wedge resulted in the concentration of deformation at the rear of the wedge and the correlative decreasing number of thrusts. As revealed by analogous models, the addition of syntectonic deposits change significantly the thickness of the thrust wedge especially in the frontal parts and allows the critical taper to be attained without forming new thrusts outside of the wedge (Storti and McClay, 1995). With regard to the Yuching section, lateral change observed in number of thrusts or the absence of some of them (Chutouchi and Lunhou thrust of Yuching section) can be related to the influence of syntectonic deposition. Beneath the Lungchuan thrust, the shortening is mainly accommodated by the internal thickening within the upper ductile décollement and by late basement deformation. To the west, the deformation propagates farther beneath the Coastal plain in favor of a flat thrust lying near 2 km.

Along the Kuanmiao section, an amount of shortening nearly 24 km is estimated from the uppermost units, which is comparable to the amount of shortening defined north of the CTFZ in the Yushing section.

4.4. Alien section

The Alien cross-section (Fig. 11) is the southernmost section of the study located south of the CTFZ (Fig. 4). This section is striking approximately N115°E parallel to the mean direction of shortening deduced from paleostress analysis and parallel to the regional transport direction. With respect to northern section structural changes occur in parallel with the disappearance of the Pingchi thrust sheet that dies out into lateral ramp outlining the southern extent of the CTFZ. The Alien section indicates that the deformation is mostly accommodated in the upper part of the Neogene sedimentary cover. This thin-skinned type of deformation is particularly clear in the western part of the section where a succession of west-verging fault-propagation folds were formed over a shallow décollement lying at 2 km within the thick mudstones of the Gutingkeng formation.

Across-strike variation of structural style is clearly emphasized and occurs abruptly across the Chishan thrust. The occurrence of a backthrust and associated east-verging fault-propagation fold is shown by seismic reflection line and gravity anomalies (Hsieh, 1970). Backthrusting in the eastern part of the section could be put into continuity with the northern pop-up structure of the Kuanmiao section (Fig. 8). The sequential deformation could be described as follow; first an inherited normal fault (the Chishan thrust) is reactivated and progressively inverted during the Neogene compression (Fig. 6); second, as the deformation increases the upper ductile décollement level is activated and backthrusting occurs at the hinge of the Chishan high-angle thrust.

With regard to the northern sections we estimate a lower total amount of shortening of nearly 13 km in the detached upper cover.

5. Tentative estimates of total and intermediate shortening rates

Preliminary dating of thrusting based on tectonosedimentary analysis (Figs. 5 and 6) and construction of balanced cross-sections (Figs. 8, 10 and 11) led to discuss the kinematics of the Southwestern Foothills in terms of shortening rates. The present-day geometry of the studied balanced cross sections mainly results from shortening along thrusts that occurred continuously throughout the evolution of the southern foreland fold-and-thrust belt.

Basically, the estimate of intermediate shortening

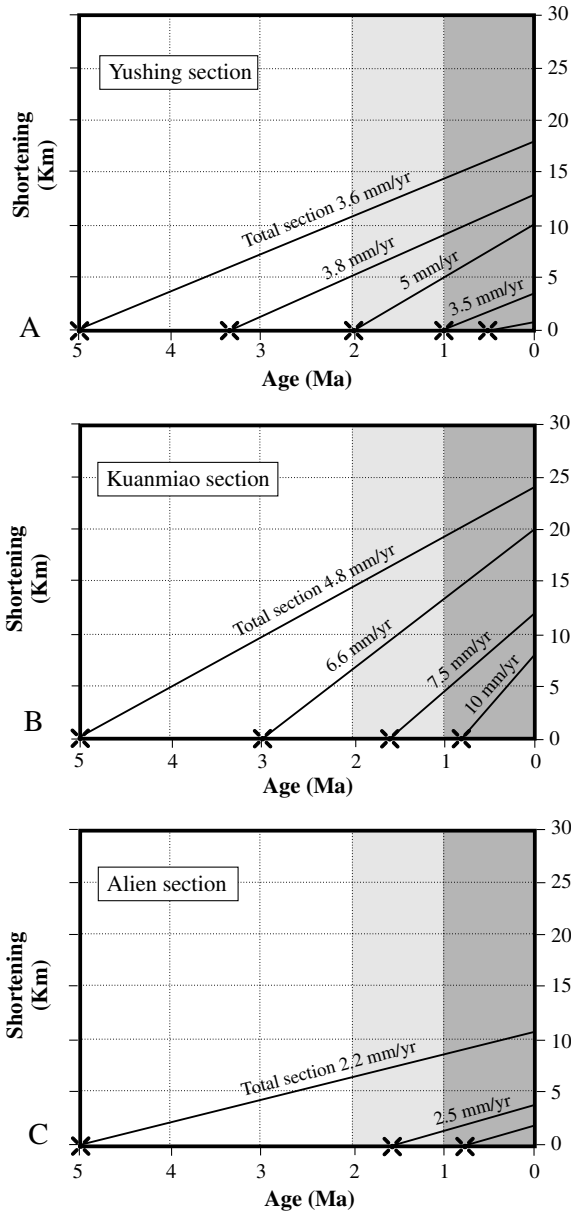

Fig. 12. Rates of shortening (plot of shortening versus time) based on the results of balancing and tectono-sedimentary study along each studied section: (A) Yushing section; (B) Kuanmiao section; (C) Alien section. Crosses (see also Fig. 6A) indicate age of local thrust initiation along each section (also refer to balanced cross-sections). Shaded areas correspond to regional tectonic stages reported in Fig. 6.

rates is provided by comparing the final and initial lengths of a given cross section balanced and restored in a considered time interval, for instance between two episodes of thrusting. This way of calculating intermediate shortening rates is strongly dependent on the accuracy of structural constraints (in space and time) on the intermediate balanced sections required to reconstruct forward (or backward) kinematics paths. Even though this method may lead to valuable results, we have chosen not to use it since it is necessary to speculate on the intermediate geometries of thrust system.

The problem of the estimate of intermediate shortening rates must be tentatively considered on the basis of three constraints: (1) the total balanced section itself, which gives the final length after contraction; (2) the pre-collisional restored cross section, which gives the initial length before contraction; and (3) the ages of thrusting, which give time constraints for estimates of the intermediate shortening rates. Consequently, the major contrast with respect to shortening rates usually estimated from intermediate restored and balanced sections, is that average rates of shortening are calculated based on the total balanced and restored cross-sections (Figs. 8, 10 and 11).

Since a particular thrust is activated, the total amount of shortening is obtained by first considering a regional pin line in the Coastal Plain which marks the position of no movement and secondly a local pin line anchored to the thrust sheet located at the back of the considered moving thrust sheet. The difference between the initial (intermediate stage) and final (present) position of the local pin line on the restored and balanced sections gives the average shortening over the considered time interval. The result combines the shortening associated with the deformation of a newly deformed thrust sheet, i.e. shortening due to displacement along the thrust plus shortening due to folding in the sheet, and the shortening undergone within the outer part of the section since the thrust was activated.

Note that during a specific stage of deformation we cannot in most cases take into account shortening accommodated at the rear of the considered moving thrust sheet: the deformation of inner thrust units is considered to be achieved when a new in-sequence thrust sheet is activated, so that this still likely

ongoing deformation is not included over the new time span considered. Consequently, such as in other methods, the inner thrust sheets are thus considered to be passively transported, which lead to underestimate the intermediate shortening rates along the section. If well-dated subsequent deformation (out-of-sequence thrusting or backthrusting) occurs at the rear, it can nevertheless be considered by estimating independently the related shortening and adding it to the intermediate amount of shortening. This may lead to overestimate of shortening rates for younger stages that follows the initiation of rearward deformation. Note that all these errors are also implicitly done in classic methods because the deformation history is unknown between specific stages.

Compared to more classical methods that introduce errors on rates of shortening from unconstrained intermediate geological sections, this present method allows first to calibrate overestimates or underestimates on rates and second to satisfactorily consider the identified structural and stratigraphic constraints obtained from the balanced and restored sections without speculating on their geometry at a given age. The results are discussed for each balanced cross-sections (Fig. 12A–C).

5.1. Yushing section

The total shortening estimated from Yushing balanced cross-section is nearly 18 km (Fig. 8). This total shortening includes both deformation in the upper cover and within the pre-Miocene strata. Deformation started during the Early Pliocene at 5 Ma contemporaneously with the initiation of the inner Chishan thrust, which is a major inherited extensional feature. Since this stage, we calculate that the Yushing section was shortened at an average rate of about 3.6 mm/year (Fig. 12A). Then, the outer Pingchi thrust is activated at 3.4 Ma (Fig. 6): since the upper Pliocene–lower Pleistocene, the section thus displays an average shortening rate of almost 3.8 mm/year, similar to rate estimated for a larger time span. Then, the Lunhou thrust is initiated at nearly 2 Ma, the shortening rate reaches 5 mm/year, slightly greater than previous estimates. At 1 Ma, since the Chutouchi out-of-sequence thrust is activated, the section is shortened at a rate of nearly 3.5 mm/year. After 0.4–0.5 Ma (initiation of the outermost Niushan thrust) the section displays a low amount of shortening leading to an estimate of the minimal shortening rate of 2.4–3 mm/year. The latter result may be explained by (1) high sediments accumulation on top of the Niushan thrust sheet and/or (2) low amount of shortening along steeply dipping thrust that results from the reactivation of extensional structures.

5.2. Kuanmiao section

Across the Kuanmiao section, we have estimated an amount of shortening of 24 km (Fig. 10). Like in the northern Yuching section, the Chishan thrust is activated at 5 Ma. We estimate an average shortening rate along the section of 4.8 mm/year since 5 Ma (Fig. 12B), which is slightly greater than the rate defined to the north. Then, the outer Pingchi thrust initiates in-sequence approximately at the same time than northward, that is near 3 Ma. Therefore, we estimate that the section was shortened since the Middle Pliocene until present at an average rate of 6.6 mm/year. In the western part of the section, the tectono-sedimentary analysis has demonstrated that deformation has begun along the Lungchuan thrust near 1.6 Ma. Consequently, taking into account the shortening accommodated in this western part of the section, we estimate an average shortening rate of 7.5 mm/year since the Middle Pleistocene. For the Meilin thrust we estimate a maximal rate of shortening of 10 mm/year since 0.8 Ma. These rates of shortening show an apparent increase of intermediate shortening rates from older to younger specific stages of deformation. Even though this result might effectively due to a true increase of deformation rates since the beginning of the collision, we must consider that rates may be overestimated due to the addition of the shortening accommodated along the Chishan backthrust in the same way for each specific stage of deformation. The maximum error done on estimate of shortening rate should not exceed 40 percent for the last stage.

5.3. Alien section

The total shortening estimated for the Alien section is approximately 11 km (Fig. 11). According to the balanced cross section, the deformation is accommodated, in a major part, along the inner Chishan thrust. Such as in the northern sections, the Chishan thrust is activated at the beginning of the collision near 5 Ma,

which lead to estimate an average shortening rate of almost 2.2 mm/year along the section (Fig. 12C). We date the Lungchuan thrust initiation at 1.6 Ma such as northward but the accommodated shortening within the frontal thrust sheets is considerably lower. Consequently, we estimate a rate of shortening since 1.6 Ma of 2.5 mm/year. Then at 0.8 Ma, numerous thrusts are activated (Gutingkeng and Meilin thrusts and Chishan backthrust): a shortening rate of 2.5 mm/year is estimated, similar to that calculated for the section since 5 Ma.

6. Conclusions

Despite evidence of an initial stage of collision in the Late Miocene near 8–12 Ma, the compressional deformation and the foreland flexure induced by the arc–continent collision were mainly initiated in the Early Pliocene at 5 Ma. Based on the tectono-sedimentary analysis three major Plio-Pleistocene deformational episodes could be determined in the southwestern Foothills:

(1) The first stage begins at 5 Ma with the onset of the Taiwan collision and initiation of the flexural subsidence. During the Pliocene, until 2–1.6 Ma, the foreland is characterized by low rates of sedimentation (<1 km/Ma) associated with a prominent shallow-marine deposition (Fig. 6). Few thrusts are active at that time (Fig. 6) and compressional deformation mainly results from the reactivation and inversion of inherited extensional features of the rifted Chinese margin such as the inner Chishan thrust (Figs. 8, 10 and 11). This setting reflects an initial submarine accretionary stage associated with moderate tectonic activity and underfilled foreland basin.

(2) The second major stage occurs in the Late Pliocene–Early Pleistocene and corresponds to a transitional stage. It is correlated with important syntectonic unconformities associated with the deposition of turbidites of the Liuchungchi and Gutingkeng formations. This "intermediate" collision stage sealed the evolution of the southern foreland thrust wedge from submarine to dominant continental depositional environment which is correlated with the increase of accumulation rates from ~0.5 to ~2 km/Ma related to the rapid exhumation and denudation of the Central Range (Fig. 6). Thrusting activity increases at that time as shown by the thrust initiation (Lunhou and Lungchuan thrusts) and reactivation (Pingchi and Chishan thrusts) (Figs. 8, 10 and 11).

(3) The last stage of deformation occurs in the Middle Pleistocene near 0.8–1 Ma. At that time the syntectonic deposition in the southern Foothills evolves progressively to brackish and fluvial facies and is characterized by high rates of sedimentation reaching 3 km/Ma. This shows the general tendency for the foreland basin to be overfilled. Most of the thrusts encountered in the southern Foothills are activated at that time or reactivated. Furthermore, out-of-sequence thrusting (Chutouchi thrust) and backthrusting occur (Chishan backthrust) (Fig. 6) indicating that deformation mostly accumulates at the rear of the thrust wedge.

The estimates of shortening rates indicate that from 5 Ma to the present the northern studied sections were shortened at rates of 3.6–4.8 mm/year (Yushing and Kuanmiao sections, respectively) and the southern section at 2.2 mm/year (Alien section) (Fig. 12).

An important result is that on average, for a given section, the total and intermediate shortening rates are more or less similar (Fig. 12). Consequently, the compressional deformation propagates continuously through time into the foreland, even though major periods of local tectonic activity have been distinguished and correlated with large-scale tectonic stages (Fig. 6). This result may confirm that long-term deformation in the Taiwan foreland thrust belt (at least in the detached cover) is more or less at steady-state since the beginning of the collision. Moreover, the shortening rates estimated in northern Yushing and central Kuanmiao sections can be considered as comparable in a first approximation. In addition, they are 40–50% greater than those calculated to the south in the Alien section. As the initiation of deformation started synchronously along the three sections (at nearly 5 Ma), the southward decrease of shortening rates in the southwestern Foothills might be related to both the influences of the Peikang indentation to the north and the southward transition, at the scale of the southwestern Foothills, from collision to subduction setting. However, the effect of obliquity of the convergence resulting in regional southward migration of the collision cannot be definitely inferred from this analysis.

To conclude, high variability occurs in nature and processes of syntectonic deposition, in structural styles and kinematics of the deformation in the southwestern Foothills. These changes are identified in time and space, along-strike and across-strike, as well with depth. Moreover, even though inherited features could have influenced the evolution of this region of the Foothills, the propagation and mechanisms of the Taiwan arc–continent collision itself, i.e. indentation in the foreland and lateral transition from collision to subduction setting, have important consequences on the kinematics and deformation in the southwestern Taiwan foreland thrust belt.

Moreover, this work raises some questions about the history of the Taiwan Mountain Range. A simple kinematic model including in-sequence emplacement of thrust belts above a single detachment (Suppe, 1980) implies that deformation and metamorphism in the Central Range is much older than the foreland thrust belt. Because we date the first record of the collision in the southwestern foreland thrust belt in the Early Pliocene, based on the sedimentary analysis, a similar age of 5 Ma for the Central Range is theoretically unrealistic based on this model. However, the flexural subsidence recorded within the foreland strongly suggests that the proposed 5 Ma age for the whole collision is correct. We therefore propose to consider a second deeper décollement level allowing shortening in the shallow wedge to occur nearly synchronous with ductile deformation and metamorphism in the deeper crust; this deeper part of the crust being secondarily exhumed as the Central Range by out-of-sequence thrusting along the Chaochou fault around 2–1.6 Ma in relation with this deeper décollement, enhancing flexural subsidence. A consistent model of shallow-related and deep-related imbricate thrust wedges has been already discussed for Taiwan (Mouthereau et al., 1999, 2001). This sequence of deformation is supported by evidence of low sedimentation/accumulation rates during the first submarine stage of the collision whereas significant increase of sedimentation/accumulation rates occurred in the Early Pleistocene synchronous with uplift of the Central Range and influx of continental deposits. The model proposed herein rather fits the recent model of Malavielle (1999) for the Arc–Continent collision in Taiwan.

Acknowledgements

This work was supported by the Institut Français à Taipei-National Science Council of Taiwan cooperation framework, the French Ministry of Research and Education and the University of Pierre et Marie Curie. Help from the Central Geological Survey of Taiwan and the Chinese Petroleum Corporation is gratefully acknowledged. The authors thank very much B. Colletta for his useful comments and help on construction of balanced cross-sections, as well as the anonymous reviewers for their constructive remarks that lead to significantly improve the manuscript.

References

Anadon, P., Cabrera, L., Colombo, F., Marzo, M., Riba, O., 1986. Syntectonic intraformational unconformities in alluvial fan deposits, eastern Ebro Basin margins (NE Spain). Spec. Publ. Int. Ass. Sediment. 8, 259–271.

Angelier, J., Barrier, E., Chu, H.T., 1986. Plate collision and paleostress trajectories in a fold-thrust belt: the Foothills of Taiwan. Tectonophysics 125, 161–178.

Angelier, J., Bergerat, F., Chu, H.T., Juang, W.S., Lu, C.Y., 1990. Paleostress analysis as a key to margin extension: the Penghu Islands, South China Sea. Tectonophysics 183, 161–176.

Beaumont, C., 1981. Foreland basins. Geophys. J. R. Astron. Soc. 65, 291–329.

Burbank, D.W., Raynolds, G.H., 1988. Stratigraphic keys to the timing of thrusting in terrestrial foreland basins: applications to the northwestern Himalaya. In: Kleinspehn, K.L., Paola, C. (Eds.). New Perspectives in Basin Analysis. Springer, New York, pp. 331–351.

Chang, L.S., Y.T., Yeh, 1981. A source model of the Paiho, Taiwan earthquake from the inversion of teleseismic body waveforms, National Science Council Report, Taiwan, 65 pp.

Chang, S.S.L., Chi, W.R., 1983. Neogene nannoplankton biostratigraphy in Taiwan and the tectonic implications. Petrol. Geol. Taiwan 19, 93–147.

Chang, Y.L., Lee, C.I., Lin, C.W., Hsu, C.H., Mao, E.W., 1996. Inversion tectonics in the Foothills of the Chiayi–Tainan area, southwestern Taiwan. Petrol. Geol. Taiwan 15, 199–217.

Chen, H., 1984. Crustal uplift and subsidence in Taiwan: an account based upon retriangulation results. Spec. Publ. Central Geol. Surv. 3, 127–140 (in Chinese).

Chi, W.R., Huang, H.M., 1981. Nannobiostratigraphy and paleoenvironments of the Late Neogene sediments and tectonic implications in the Miaoli area, Taiwan. Petrol. Geol. Taiwan 18, 111–143.

Chinese Petroleum Corporation, 1989. Geological maps of Tainan, scale 1:100000, 1 sheet.

Covey, M., 1984. Lithofacies analysis and basin reconstruction,

Plio-Pleistocene western Taiwan Foredeep. Petrol. Geol. Taiwan 20, 53–83.

Covey, M., 1986. The evolution of foreland basins to steady state: evidence from the western Taiwan foreland basin. In Allen, P.A., Homewood, P. (Eds.), Foreland Basins, Spec.Publ. Int. Ass. Sediment., 8, pp. 7–90.

Colletta, B., Letouzey, J., Soares, J., Specht, M., 1999. Detachment versus fault-propagation folding: insights from the sub-Andean Ranges of southern Bolivia, Thrust Tectonics Conference, Royal Holloway of London, 26–29 April, pp. 106–109.

Davis, D., Suppe, J., Dahlen, F.A., 1983. Mechanisms of fold-and-thrust belts and accretionary wedges. J. Geophys. Res. 88, 1153–1172.

Deffontaines, B., Lacombe, O., Angelier, J., Chu, H.T., Mouthereau, F., Lee, C.T., Déramond, J., Lee, J.F., Yu, M.S., Liew, P.M., 1997. Quaternary transfer faulting in the Taiwan Foothills: evidence from a multisource approach. Tectonophysics 274, 61–82.

Delcaillau, B., Angelier, J., Herail, G., Chu, H.T., Lee, J.C., Liew, P.M., Lin, T.S., Lu, C.Y., Teng, L., Deramond, J., Souquet, P., 1993. Evolution morphostructural et sédimentaire d'un bassin d'avant-pays en régime de collision oblique: le Piémont occidental de Taiwan. C. R. Acad. Sci. Paris 315 (II), 1239–11244.

Déramond, J., Delcaillau, B., Souquet, P., Angelier, J., Chu, H.T., Lee, J.F., Lee, T.Q., Liew, P.M., Lin, T.S., Teng, L., 1996. Signatures de la surrection et de la subsidence dans les bassins d'avant-chaîne actifs: les Foothills de Taiwan (de 8 Ma à l'Actuel). Bull. Soc. Geol. France 167 (1), 111–123.

Eason, H., 1997. Evolution of the Pliocene to Pleistocene sedimentary environments in an arc–continent collision zone: evidence from the analyses of lithofacies and ichnofacies in the southwestern foothills of Taiwan. J. Asian Earth Sci. 15 (4/5), 381–392.

Ellwood, A., Wang, C.Y., Teng, L.S., Yen, H.Y., 1996. Gravimetric examination of thin-skinned detachment vs basement-involved models for the Taiwan orogen. J. Geol. Soc. China 39 (2), 209–221.

Flemings, P.B., Jordan, T.E., 1989. A synthetic stratigraphic model of foreland basin development. J. Geophys. Res. 94, 3851–3866.

Ho, C.S., 1988. An introduction to the geology of Taiwan: explanatory text of the geological map of Taiwan, 2nd ed., Central Geol. Surv., 192 pp.

Horng, C.S., Shea, K.S., 1994. Study of nannofossil biostratigraphy in the eastern part of the Erhjen-chi section, southern Taiwan. Spec. Publ. Central Geol. Surv. 8, 181–204.

Hsieh, S.H., 1970. Geology and gravity anomalies of the Pingtung plain, Taiwan. Proc. Geol. Soc. China 13, 76–89.

Hsiao, P.T., 1974. Subsurface geologic study of the Hsinying Coastal Plain area, Taiwan. Petrol. Geol. Taiwan 11, 27–39.

Hu, C.C., Sheen, H.C., 1989. An evaluation of the hydrocarbon potential of the Niushan and Lungtien structures in the Tainan area. Petrol. Geol. Taiwan 25, 11–34.

Huang, B.S., Chen, K.C., Yeh, Y.T., 1996. Source parameters of the December 15, 1993 Tapu earthquake from first-P motions and waveforms. J. Geol. Soc. China 39 (3), 235–250.

Hung, J.H., Wiltshko, D.V., Lin, H.C., Hickman, J.B., Fang, P., Bock, Y., 1999. Structure and motion of the southwestern Taiwan fold and thrust belt. TAO 10 (3), 543–568.

Jordan, T.E., Flemings, P.B., 1991. Large-scale stratigraphic architecture, eustatic variation, and unsteady tectonism: a theoretical evaluation. J. Geophys. Res. 96, 6681–6699.

Kao, H., Shen, S.H., Ma, K.F., 1998. Transition from oblique subduction to collision: Earthquakes in the southern Ryukyu arc–Taiwan region. J. Geophys. Res. 103, 7211–7229.

Lacombe, O., Angelier, J., Chen, H.W., Deffontaines, B., Chu, H.T., Rocher, M., 1997. Syndepositional tectonics and extension–compression relationships at the front of the Taiwan collision belt: a case study in the Pleistocene reefal limestones of Kaohsiung (SW Taiwan). Tectonophysics 274, 83–96.

Lacombe, O., Mouthereau, F., Deffontaines, B., Angelier, J., Chu, H.T., Lee, C.T., 1999. Geometry and quaternary kinematics of fold-and-thrust units of SW Taiwan. Tectonics 18 (6), 1198–1223.

Lacombe, A., Mouthereau, F., Angelier, J., Deffontaines, B., 2001. Structural, geodetic and seismological evidence for tectonic escape in SW Taiwan. Tectonophysics 333 (1/2), 323–345.

Lee, P.J., 1977. Rate of the Early Pleistocene uplift in Taiwan. Mem. Geol. Soc. China 2, 71–76.

Lee, T.Y., Tang, C.H., Ting, J.S., Tseng, C.S., 1993. Sequence stratigraphy of the Tainan basin, offshore southwestern Taiwan. Petrol. Geol. Taiwan 28, 119–158.

Lu, C.Y., Hsü, K.J., 1992. Tectonic evolution of the Taiwan mountain belt. Petrol. Geol. Taiwan 27, 15–35.

Ma, K.F., Chen, J.Y., 1999. Focal mechanism determination of the 1991 Chiali Earthquake (Ml = 5.7) Sequence. TAO 10 (2), 447–470.

Ma, K.F., Lee, C.T., Tsai, Y.B., 1999. The Chi-chi earthquake: large surface displacements on an inland thrust fault. EOS 80 (50), 605.

Malavielle, J., 1999. Evolutionary model for arc–continent collision in Taiwan. Active subduction and collision in southeast Asia: data and models, International Conference and Fourth France–Taiwan Symposium, Montpellier, Mai, p. 231.

Mouthereau, F., Angelier, J., Deffontaines, B., Lacombe, O., Chu, H.T., Colletta, B., Déramond, J., Yu, M.S., Lee, J.F., 1996. Cinématique actuelle et récente du front de chaîne de Taiwan. C. R. Acad. Sci. Paris 323 (II), 713–719.

Mouthereau F., Deffontaines, B., Lacombe, O., Angelier, J., 1999. Basement control on structural style, wedge geometry and kinematics at the front of Taiwan mountain belt, Thrust Tectonics 99, London, April, p. 270.

Mouthereau, F., Deffontaines, B., Lacombe, O., Angelier, J., 2001. Along-strike variations of the Taiwan belt front: basement control on structural style, wedge geometry and kinematics. GSA Spec. Bull. (in press).

Moretti, I., Larrere, M., 1989. LOCACE, computer-aided construction of balanced geological cross section. Geobyte, 16–24.

Namson, J., 1981. Structure of the western foothills belt, Miaoli-Hsinchu area, Taiwan: (I) southern part. Petrol. Geol. Taiwan 18, 31–51.

Oinomikado, T., (955. Micropaleontological investigation of the Chishan standard section, near Tainan, Taiwan. Chin. Petrol. Corp. Paleontol., Lab. Rept, 7, 10 pp.

Pautot, G., Rangin, C., Briais, A., Tapponnier, P., Beuzart, P.,

Lericolais, G., Mathieu, X., Wu, J., Han, S., Li, H., Lu, Y., Zhao, J., 1986. Spreading direction in the Central South China Sea. Nature 321 (6066), 150–154.

Puigedefabregas, C., Munoz, J.A., Verges, J., 1992. Thrusting and foreland basin evolution in the southern Pyrenees. In: McClay, K.R. (Ed.). Thrust Tectonics. Chapman and Hall, London, pp. 93–104.

Rau, R.J., Wu, F.T., 1998. Active tectonics of Taiwan orogeny from focal mechanisms of small-to-moderate sized earthquakes. TAO 9 (4), 755–778.

Riba, O., 1976. Syntectonic unconformities of the Alto Cardener, Spanish Pyrenees: a genetic interpretation. Sediment. Geol. 15, 213–233.

Rocher, M., Lacombe, O., Angelier, J., Chen, H.W., 1996. Mechanical twin sets in calcite as markers of recent collisional events in fold-and-thrust belts: evidence from the reefal limestones of SW Taiwan. Tectonics 15 (5), 984–996.

Roure, F., Howell, D.G., Guellec, S., Casero, P., 1990. Shallow structures induced by deep-seated thrusting. In: Letouzey, J. (Ed.), Petroleum and Tectonics in Mobile Belts, Technip, pp. 15–30.

Sinclair, H.D., 1997. Flysch to molasses transition in peripheral foreland basins: the role of the passive margin versus slab breakoff. Geology 25, 1123–1126.

Shaw, C.L., 1996. Stratigraphic correlation and isopachs maps of the western Taiwan Basin. TAO 7 (3), 333–360.

Storti, F., McClay, K., 1995. Influence of syntectonic sedimentation on thrust wedges in analogue models. Geology 23, 999–1002.

Suppe, J., 1976. Décollement folding in southwestern Taiwan. Petrol. Geol. Taiwan 13, 25–35.

Suppe, J., Namson, J., 1979. Fault-bend origin of frontal folds of the western Taiwan fold-and-thrust belt. Petrol. Geol. Taiwan 16, 1–18.

Suppe, J., 1980. Imbricated structure of western foothills belt, southcentral Taiwan. Petrol. Geol. Taiwan 17, 1–16.

Suppe, J., 1981. Mechanics of mountain-building and metamorphism in Taiwan. Mem. Geol. Soc. China 4, 67–90.

Suppe, J., 1983. Geometry and kinematics of fault-bend folding. Am. J. Sci. 283, 684–721.

Suppe, J., 1984. Kinematics of arc–continent collision, flipping of subduction, and back-arc spreading near Taiwan. Mem. Geol. Soc. China 6, 21–34.

Teng, L.S., 1990. Geotectonic evolution of the Late Cenozoic arc–continent collision in Taiwan. Tectonophysics 183, 57–76.

Wu, F.T., Rau, R.J., Salzberg, D., 1997. Taiwan orogeny: thin-skinned or lithospheric collision. Tectonophysics 274, 191–220.

Yen, H.Y., Yeh, Y.H., Wu, F.T., 1998. Two-dimensional crustal structures of Taiwan from gravity data. Tectonics 17, 104–111.

Yu, H.S., Chou, Y.W., 1999. Characteristics and development of the flexural forebulge and basal unconformity of western Taiwan foreland basin, active subduction and collision in Southeast Asia: data and models, International Conference and Fourth France–Taiwan Symposium, Montpellier, Mai, p. 69.

Yu, M.S., L.S. Teng, 1988. Neogene–Quaternary basin subsidence of northwestern Taiwan as revealed by geohistory, Proc. Second Taiwan Symp. Geophys., pp. 355–363.

Yu, S.B., Chen, H.Y., Kuo, L.C., 1997. Velocity field of GPS stations in the Taiwan area. Tectonophysics 274, 41–59.

Yu, S.B., Kuo, L.C., Punongbayan, R.S., Ramos, E.G., 1999. GPS observation of crustal deformation in the Taiwan–Luzon region. Geophys. Res. Lett. 26, 923–926.